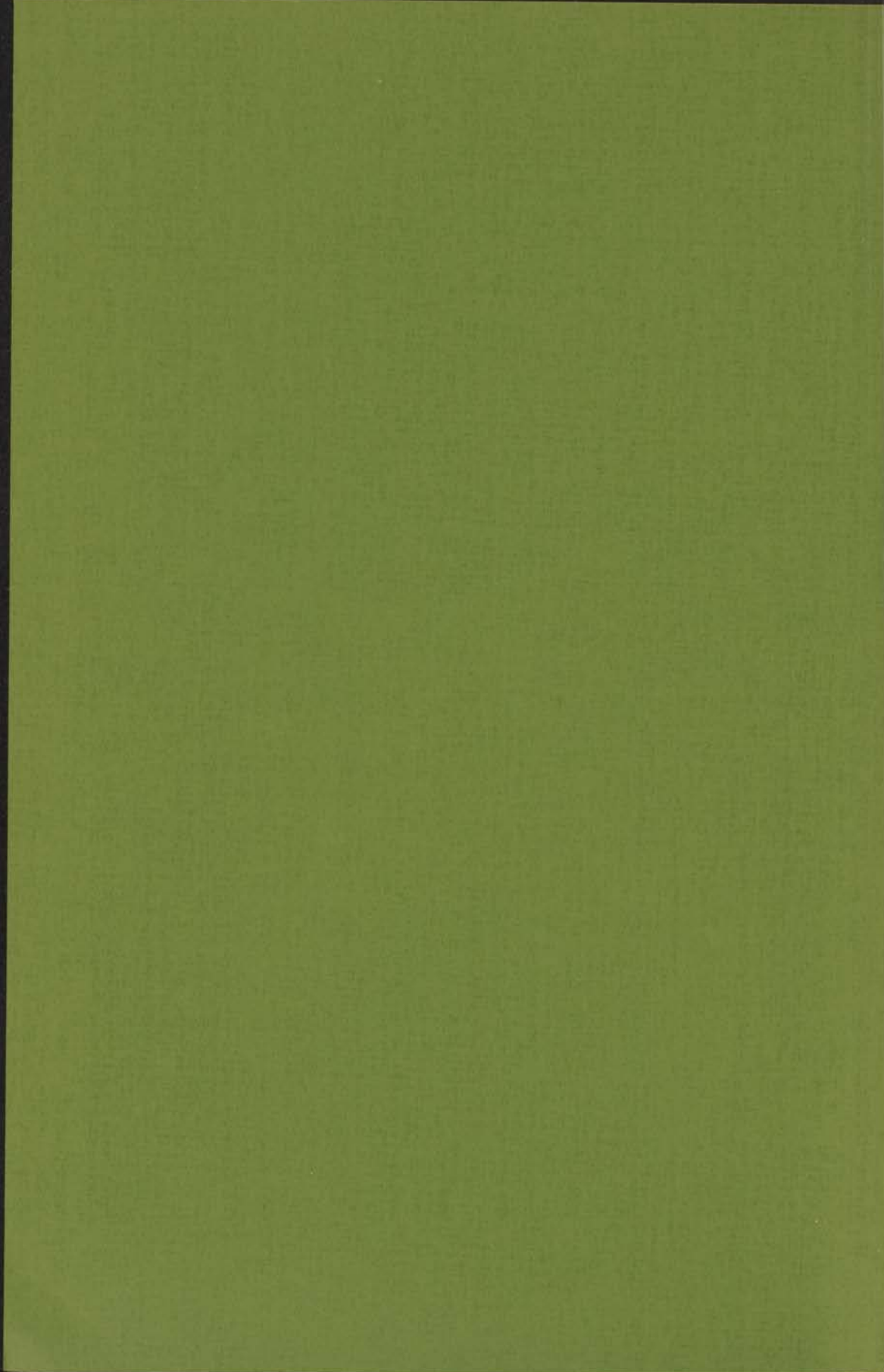


p. 26 te lezen
Eusebe p. 22 e 23

HARD PHOTON CORRECTIONS FOR PROCESSES
IN e^+e^- COLLIDING BEAM EXPERIMENTS

INSTITUUT LORENZ
voor theoretische natuurkunde
Nieuwsteeg 18-Lelystad, Nederland

K. J. F. GAEMERS



13 JUNI 1974

HARD PHOTON CORRECTIONS FOR PROCESSES

IN e^+e^- COLLIDING BEAM EXPERIMENTS

PROEFSCHRIFT

TER VERKRIJGING VAN DE GRAAD VAN DOCTOR IN
DE WISKUNDE EN NATUURWETENSCHAPPEN AAN DE
RIJKSUNIVERSITEIT TE LEIDEN, OP GEZAG VAN DE
RECTOR MAGNIFICUS DR. A.E. COHEN, HOOGLEERAAR

IN DE FACULTEIT DER LETTEREN, VOLGENS
BESLUIT VAN HET COLLEGE VAN DEKANEN TE
VERDEDIGEN OP DONDERDAG 27 JUNI 1974

TE KLOKKE 15.15 UUR

door

KAREL JOHANNES FREDERIK GAEMERS

geboren te Den Haag in 1944

INSTITUUT LORENTZ

voor theoretische natuurkunde
Nieuwsteeg 18-Leiden-Nederland

kast dissertaties

PROMOTOR: PROF. DR. J.A.M. COX

Dit proefschrift kwam tot stand mede onder leiding van
DR. F.A. BERENDS

S T E L L I N G E N

- I. Het door Borchers ontwikkelde algebraïsche formalisme, dat door hem wordt toegepast in de relativistische quantum velden theorie, kan in gegeneraliseerde vorm gebruikt worden om willekeurige klassieke en quantum mechanische systemen te karakteriseren.
 H. Borchers, Nuov. Cim. 24 (1962), 214.
- II. Het is mogelijk om in de quantum veldentheorie een definitie te geven van normaalproduct die geen gebruik maakt van een splitsing in creatie- en annihilatie operatoren. Het is waarschijnlijk dat deze definitie gebruikt dient te worden in de bewegingsvergelijkingen voor gekoppelde velden.
 R. Stora, Les Houches 1971.
- III. In een Wightman veldentheorie met "mass gap" kunnen de asymptotische vrije velden gegeven worden zonder de limietprocedure van D. Ruelle te gebruiken.
 D. Ruelle, Helv. Phys. Acta 35 (1962), 147.
- IV. Ten onrechte wekt H. Weyl het vermoeden dat de Hilbertruimte van kwadratisch integreerbare functies op de eenheidsirkel een niet separabele ruimte is.
 H. Weyl, The Theory of Groups and Quantum Mechanics, p.32 Dover Publications Inc.
- V. Meting van de differentiele werkzame doorsnede van de reactie $e^+e^- \rightarrow \pi^+\pi^-$ kan belangrijke informatie geven over boson resonanties met $C = +1$, mits de lading van de uitgaande deeltjes gedetecteerd wordt.
- VI. Bij de berekening van fysische grootheden in het eendimensionale X-Y model geven de a-cyclische en c-cyclische randvoorwaarden, zelfs in de thermodynamische limiet, niet altijd hetzelfde resultaat.

VII. Om de resultaten van e^+e^- "colliding beam" experimenten goed te interpreteren is een nauwkeurige analyse van de experimentele situatie, i.h.b. van de meetnauwkeurigheid, noodzakelijk.

Hoofdstuk III van dit proefschrift.

VIII. De techniek die D. Yennie et al. gebruiken om te bewijzen dat werkzame doorsneden in de quantum electrodynamica niet negatief worden bij grote meetnauwkeurigheid, is niet bruikbaar voor numerieke berekeningen.

D.R. Yennie, S.C. Frautschi and H. Suura, Ann. Phys. (N.Y.) 13 (1961), 379.

IX. De suggestie van Y. Tokunaga et al. dat de door hen waargenomen relaxatieverschijnselen in $\text{NiTi}_2(\text{SO}_4)_2 \cdot 6\text{H}_2\text{O}$ toegeschreven moeten worden aan het directe proces is onjuist.

Y. Tokunaga et al., Journ. Phys. Soc. Japan 35 (1973), 1353.

X. Het teken van de ladings asymmetrie in de reactie $e^+e^- \rightarrow \mu^+\mu^-$ kan eenvoudig kwalitatief verklaard worden.

K.J.F. Gaemers

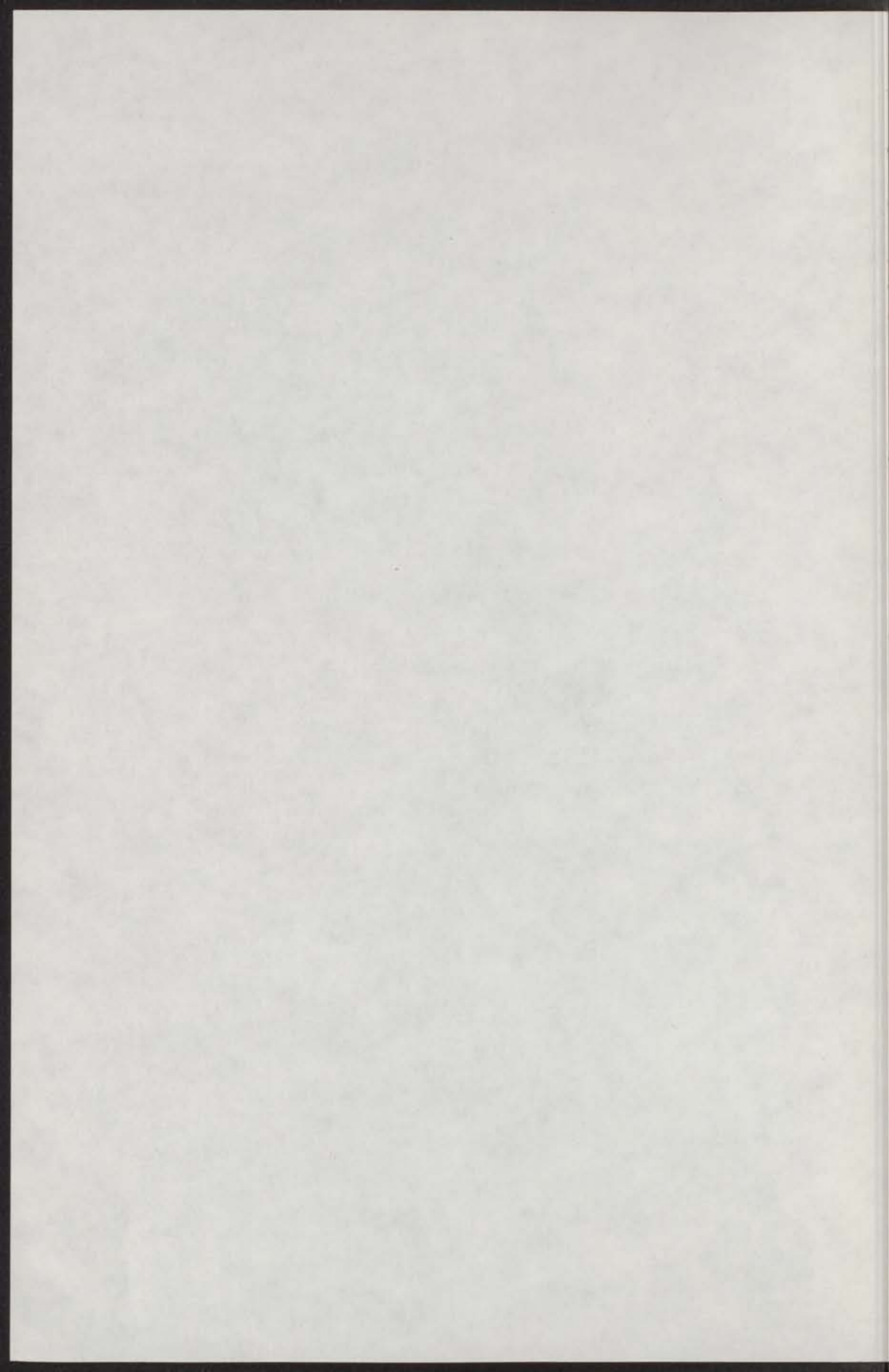
27 juni 1974

CONTENTS

I.	INTRODUCTION	3
II.	ISSUE OF QUANTUM ELECTRODYNAMICS AND e^+e^- COLLIDING BEAM EXPERIMENTS	7
	1. Issue of quantum electrodynamics	7
	2. Lowest order cross sections	8
	3. General remarks on radiative corrections	10
	4. Discussion of possible experimental situations	12
	5. Validity of the order α^2 approximation	13
III.	INDICATIVE CALCULATIONS FOR PROCESSES OCCURRING IN e^+e^- COLLIDING BEAM EXPERIMENTS	14
	1. Summary	14
	2. Kinematics and the lowest order amplitudes for $e^+e^- \rightarrow \mu^+\mu^-$	14
	3. The vertex corrections	27
	4. The vacuum polarization corrections	28
	5. The two photon exchange contributions	28
	6. The inelastic reaction	32
	7. Two photon and acyclotrons	33
	8. Mixed scattering and two gamma production	33
IV.	NUMERICAL RESULTS AND DISCUSSIONS	39
	1. Summary	39
	2. Muon scattering	40
	3. Muon pair production	44
	4. Two gamma production	44
	5. Conclusions	47
	APPENDIX A	48
	APPENDIX B	55
	APPENDIX C	55
	APPENDIX D	57
	REFERENCES	59
	RESUME	60

Aan mijn ouders

Aan mijn vrouw



C O N T E N T S

I.	INTRODUCTION	6
II.	TESTS OF QUANTUM ELECTRODYNAMICS AND e^+e^- COLLIDING BEAM EXPERIMENTS	7
	1. Tests of quantum electrodynamics	7
	2. Lowest order cross sections	8
	3. General remarks on radiative corrections	10
	4. Discussion of possible experimental situations	12
	5. Validity of the order α^3 approximation	13
III.	RADIATIVE CORRECTIONS FOR PROCESSES OCCURRING IN e^+e^- COLLIDING BEAM EXPERIMENTS	14
	1. Summary	14
	2. Kinematics and the lowest order amplitude for $e^+e^- \rightarrow \mu^+\mu^-$	14
	3. The vertex corrections	17
	4. The vacuum polarisation corrections	21
	5. The two photon exchange contributions	26
	6. The inelastic reaction	27
	7. Phase space and acoplanarity	31
	8. Bhabha scattering and two gamma production	37
IV.	NUMERICAL RESULTS AND DISCUSSIONS	39
	1. Summary	39
	2. Bhabha scattering	40
	3. Mu-pair production	44
	4. Two gamma production	46
	5. Conclusions	47
	APPENDIX A	49
	APPENDIX B	55
	APPENDIX C	65
	APPENDIX D	67
	REFERENCES	68
	SAMENVATTING	69

CHAPTER I

INTRODUCTION

I. With the advent of e^+e^- colliding beam facilities, more refined tests of quantum electrodynamics have become possible [1]. As a consequence it has become necessary to calculate more accurate theoretical cross sections for the reactions:

$$e^+e^- \rightarrow \gamma\gamma, \quad (1)$$

$$e^+e^- \rightarrow e^+e^-, \quad (2)$$

$$e^+e^- \rightarrow \mu^+\mu^-. \quad (3)$$

In this thesis theoretical cross sections for these reactions are given to order α^3 , α being the fine structure constant. These cross sections contain parts where an extra photon is emitted (bremsstrahlung). The latter contributions are very much dependent on the experimental set-up and the procedure of analyzing the data. Therefore great care has been given in handling these terms without approximation.

For realistic experimental situations, numerical calculations have been made.

The outline of this thesis is as follows. In chapter II a general discussion on the role of quantum electrodynamics in colliding beam experiments is given. Also the radiative corrections are discussed. In chapter III we describe the analytic calculations of the virtual radiative corrections and the general formalism to handle hard photons. In chapter IV numerical results are presented. Also recent experimental results will be given and compared with the theoretical calculations [2]. Finally in several appendices Feynman rules and detailed calculations for the process $e^+e^- \rightarrow \mu^+\mu^-$ are given.

CHAPTER II

TESTS OF QUANTUM ELECTRODYNAMICS AND e^+e^- COLLIDING BEAM EXPERIMENTS

II.1. Tests of quantum electrodynamics.

In studying scattering and decay processes of elementary particles it has become apparent that there are at least three classes of interactions i.e. strong, electromagnetic and weak. The other known interaction, the gravitational interaction, has not been observed directly in elementary processes in contrast to the other three. At present we have the best theoretical understanding of the electromagnetic interaction.

Of all known particles, electrons, muons and photons do not participate directly in strong interactions, so that electromagnetic interactions can be studied practically without contamination of other interactions, by looking at reactions involving only these three kinds of particles. In most cases effects of weak interaction may be neglected compared with those of electromagnetic interactions.

On the basis of quantum field theory most quantities concerning the behaviour of electrons, muons and photons can be calculated with arbitrary precision as a perturbation series in the fine structure constant $\alpha (\approx 1/137)$. This theory is called quantum electrodynamics (Q.E.D.).

Since the calculational rules of Q.E.D. were established, no essential modification of the theory has taken place. A description of Q.E.D. and general quantum field theory can be found in many textbooks [3]-[5]. With a few minor modifications we shall use conventions and Feynman rules as stated in the books by Bjorken and Drell^{*}). For convenience of reference, conventions and rules are explicitly given in appendix A.

Quantities which can be calculated in the framework of Q.E.D. and which can be put to experimental tests, fall apart into two categories. The first

^{*}) For the photon field the Gupta-Bleuler formalism was used instead of the formalism used by Bjorken and Drell where the radiation gauge is employed.

category encompasses the anomalous magnetic moments of the electron and muon, and various level shifts in atomic systems (Lamb shift). These effects are referred to as static quantities. A survey of these effects and a comparison between experimental results and theoretical predictions may be found in a review article by B.E. Lastrup et al. [6]. The second category consists of cross sections for scattering processes where the particles involved are electrons, muons and photons.

There are of course many such reactions like e.g. electron Compton scattering ($\gamma e^- \rightarrow \gamma e^-$) and Møller scattering ($e^- e^- \rightarrow e^- e^-$). In principle, reactions such as these can be used to test Q.E.D. In practice however one has to take into account the feasibility of performing accurate cross section measurements for a specific reaction on the one hand and of performing reliable theoretical calculations on the other hand^{*}).

Around 1960 the following reactions were proposed to test Q.E.D.,

$$e^+ e^- \rightarrow \gamma \gamma, \quad (1)$$

$$e^+ e^- \rightarrow e^+ e^-, \quad (2)$$

$$e^+ e^- \rightarrow \mu^+ \mu^-. \quad (3)$$

At present, experiments of this type have been performed in many laboratories by means of $e^+ e^-$ colliding beams [1],[2]. In these experiments, electrons and positrons describe a circular orbit in opposite directions. They are forced to move like this under the influence of a constant magnetic field perpendicular to the orbit. At well-defined places along the circle one lets the electron and positron beams collide (hence the name). The enormous advantage of this type of experiment is the possibility to study reactions at a center of mass energy which cannot be reached in another way, combined with the fact that the reaction rate can be made high enough so that good statistics are obtained.

II.2. Lowest order cross sections.

We will now give the lowest order cross sections for reactions (1), (2) and (3) and mention various aspects of their behaviour with angle and energy^{**}).

^{*}) Most theoretical calculations in Q.E.D. although straightforward are of considerable complexity. Many theoretical results existing in the literature contain calculational errors and/or misprints.

^{**}) In all expressions in this section, where possible the relativistic limit has been taken, i.e. terms of order m/E are neglected.

$$a. \quad e^+(p_+) + e^-(p_-) \rightarrow \gamma(q_1) + \gamma(q_2)$$

In lowest order this process gets contributions from two Feynman diagrams (fig. 1). Using standard procedures one arrives at the following expression

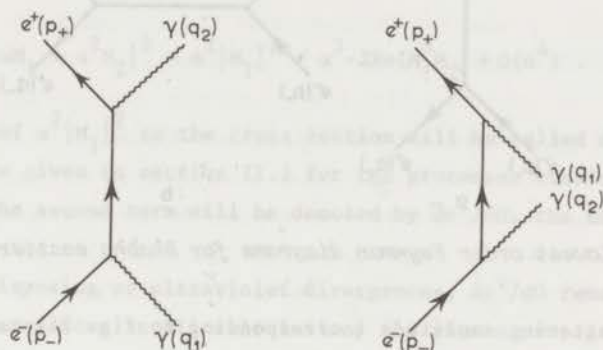


Fig. 1 Lowest order Feynman diagrams for two gamma production.

for the differential cross section,

$$\frac{d\sigma}{d\Omega_1}^0 = \frac{\alpha^2}{s} \left[\frac{2 + \sin^2\theta}{1 - \beta^2 \cos^2\theta} - \frac{2\sin^4\theta}{(1 - \beta^2 \cos^2\theta)^2} \right] \quad (4)$$

In this formula, α is the fine structure constant, s the square of the center of mass energy, β is the velocity of the incoming electrons (and positrons) and finally, θ is the angle between \vec{p}_+ and \vec{q}_1 in the center of mass system. This cross section is symmetric around $\theta = 90^\circ$ and exhibits strong peaking in the forward and backward direction. Note however that even at $\theta = 0^\circ$ and $\theta = 180^\circ$ it remains finite.

$$b. \quad e^+(p_+) + e^-(p_-) \rightarrow e^+(q_+) + e^-(q_-)$$

In lowest order, this process gets contributions from two Feynman diagrams (fig. 2), giving rise to a lowest order cross section

$$\frac{d\sigma}{d\Omega_+}^0 = \frac{\alpha^2}{2s} \left[\frac{1 + \cos^4(\theta/2)}{\sin^4(\theta/2)} - \frac{2\cos^4(\theta/2)}{\sin^2(\theta/2)} + \frac{1}{2}(1 + \cos^2\theta) \right] \quad (5)$$

The meaning of α and s is the same as under a), θ is now the angle between \vec{p}_+ and \vec{q}_+ . This cross section diverges in the forward direction; as a consequence also the total cross section is infinite. This has to be expected as

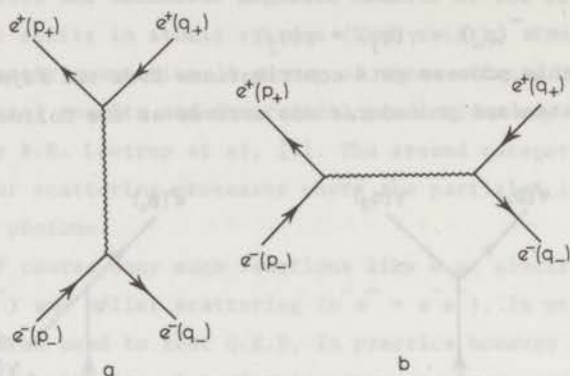


Fig. 2 Lowest order Feynman diagrams for Bhabha scattering.

part of the scattering amplitude (corresponding to fig. 2a) can be regarded as the amplitude for Coulomb scattering.

$$c. \quad e^+(p_+) + e^-(p_-) \rightarrow \mu^+(q_+) + \mu^-(q_-)$$

In lowest order we have only one diagram (fig. 3) resulting in the cross section

$$\frac{d\sigma}{d\Omega_+} = \frac{\alpha^2}{2s} \beta_\mu \left[\frac{1}{2}(1 + \cos^2 \theta) + \frac{2\mu^2}{s} (1 - \cos^2 \theta) \right]. \quad (6)$$

In this formula, μ is the muon mass and β_μ is the velocity of the outgoing muons. The threshold for this reaction is $s_{th} = 4\mu^2$. This cross section has a smooth angular behaviour. The total cross section behaves as s^{-1} for large s .

II.3. General remarks on radiative corrections.

In view of the numerical value of α , one could expect that the order α^3 contributions to the cross sections for reactions (1)-(3) are of the order of 1% of the basic cross sections. It is known however, that corrections of the order of 10% can be reached. Therefore if one wants to compare experimental cross sections with theoretical ones with an accuracy of 1% it is necessary to calculate the theoretical cross sections at least up to order α^3 . For the processes (1), (2) and (3) the order α^3 contributions to the cross section have been calculated (for details see chapter III).

In calculating the first order corrections to the basic cross sections one encounters the divergence difficulties of any relativistic quantum field theory (i.e. ultraviolet divergences), supplemented by divergences inherent to the presence of massless particles (photons), the so-called infrared divergences.

The elimination of these infrared divergences has important consequences for the radiative corrections, as we will indicate.

The quantity of interest for cross section calculations is the modulus squared of the scattering amplitude M . As the amplitude itself is given as a power series in e (the charge of the electron) we find up to order α^3 ($\alpha = e^2/4\pi$)

$$|M|^2 = |\alpha M_1 + \alpha^2 M_2|^2 = \alpha^2 |M_1|^2 + \alpha^3 \cdot 2\text{Re}(M_1^* M_2) + O(\alpha^4) . \quad (7)$$

The contribution of $\alpha^2 |M_1|^2$ to the cross section will be called $d\sigma^0/d\Omega$, these order α^2 terms are given in section II.2 for the processes considered. The contribution of the second term will be denoted by $d\sigma'/d\Omega$, the third term will be omitted.

Even after disposing of ultraviolet divergences, $d\sigma'/d\Omega$ remains infrared divergent. If one replaces in all calculations the photon propagator by $-ig_{\mu\nu}/(k^2 - \lambda^2 + i\epsilon)$ the expression for $d\sigma'/d\Omega$ will be of the form

$$A \log \frac{\lambda}{m} + B + O(\lambda) , \quad (8)$$

thus exhibiting the singularity at $\lambda = 0$. It seems that the order α^3 contributions are infinite. A solution to this problem has been given in a basic paper by Bloch and Nordsieck [7], a general analysis has been given by Yennie, Frautschi and Suura [8].

The basis for the solution of the problem is the observation that in every scattering process where charged particles are involved, extra bremsstrahlung photons are produced whose energy may be arbitrarily small. In an experimental situation it is impossible to observe all the emitted extra photons, so that the cross sections for these processes have to be added to the "elastic" cross section. Here we call elastic the process without extra photon emission. If we follow this procedure we find that to order α^3 one can have the basic process with one extra photon. Apart from $d\sigma^0/d\Omega$ and $d\sigma'/d\Omega$ we thus have a third contribution,

$$\frac{d\sigma^B}{d\Omega} = \int \frac{\partial \sigma^B}{\partial \Omega \partial \vec{k}} d^3 k . \quad (9)$$

In this expression $\partial \sigma^B / \partial \Omega \partial \vec{k}$ is the multi differential cross section where the observed final particle is detected within solid angle $d\Omega$ around a fixed direction and where the extra photon has momentum in a region $d^3 k$ around \vec{k} . The integration in (9) has to be performed over those photon momenta where this

photon is experimentally unobserved.

It turns out that the integral (9) diverges at the point $\vec{k} = 0$, a divergence which can be exhibited by taking in intermediate calculations the photon mass to be λ . If ΔE is an energy limit such that photons are not detected if their energy is smaller than ΔE , expression (9) is of the form

$$A \ln \frac{\Delta E}{\lambda} + C + O(\lambda) \quad (10)$$

Here A is the same function of the kinematical variables as the function A used in (9).

The cross section up to order α^3 can now be written as

$$\frac{d\sigma}{d\Omega} = \frac{d\sigma^0}{d\Omega} + \frac{d\sigma'}{d\Omega} + \int \frac{\partial \sigma^B}{\partial \Omega \partial \vec{k}} d^3k \quad (11)$$

As can be seen from (8), (9) and (10), in this sum the limit $\lambda \rightarrow 0$ can be taken without any problem and the order α^3 cross section is a finite and well-defined expression.

In order to give numerical results, one defines a correction factor δ_T by

$$\frac{d\sigma^0}{d\Omega} (1 + \delta_T) = \frac{d\sigma^0}{d\Omega} + \frac{d\sigma'}{d\Omega} + \int \frac{\partial \sigma^B}{\partial \Omega \partial \vec{k}} d^3k \quad (12)$$

In this way δ_T is considered as a correction to the basic cross section, a so-called radiative correction.

II.4. Discussion of possible experimental situations.

It is now obvious that the calculation of the cross section to order α^3 requires a knowledge of the experimental situation in order to calculate the integral appearing in (12). Unfortunately realistic experimental situations do not provide direct information on the momentum range of the undetected photons.

As an approximation one often assumes that in the laboratory system the photons with energy smaller than some value ΔE are undetected. If now ΔE is small enough one can perform the integration (9) analytically, provided some approximations (known as soft photon approximation) are made. Although this procedure solves the infrared problem the assumption involved is not very realistic.

Experimentally when measuring the reactions (1)-(3), one uses some criterion to decide whether the observed pair of final state particles belongs to one of

reactions (1)-(3). One can imagine two rather distinct possibilities.

In the first place, if the two final state particles are detected and their energies lie in the range $[E - \epsilon, E]$, then one counts them as real events. (E is the energy per beam.) In the second place one may select the final state particles by the criterion that they are produced back to back. Then no energy is measured, but it is established that their tracks make an angle $\delta < \zeta$, where the quantity ζ is the given maximum acollinearity. If accidentally one also sees the "undetected" photon, one has to add this event to the cross section.

We will outline a method by means of which the influence of these experimental conditions on the photon phase space can be analyzed without using the soft photon approximation. In this way the order α^3 contributions are calculated for reactions (1)-(3). Although the calculations for reaction (1) have been published by Berends and Gastmans their results will be included here for completeness [9].

II.5. Validity of the order α^3 approximation.

As can be seen from (8) and (11), the correction factor δ contains a term which behaves like $\log(\Delta E/m)$. From this we see that for very small ΔE , the corrections may become large. Also in the more realistic treatment of the external photon it remains true that if the phase space available for the photon is made very small, the corrections become large. From the full expressions it can be seen that the contribution to δ_T from terms like $\log(\Delta E/m)$ has the same sign as this logarithm so that we have the paradoxical result that for small ΔE the cross section to order α^3 may become negative. It has been shown that in cases where photon phase space is so small that this is the case, still higher order terms in α are necessary to prevent the cross section from becoming negative [8]. In other words there is an interplay between the measuring accuracy and the required order in α to which one has to do the calculations.

At present it is not known what the quantitative relation is between the volume of photon phase space and the necessary order of α . The only thing that may be said is that if theory and experiment do not agree in situations where the corrections δ_T are large and negative, one first has to take into account higher order corrections before concluding at a breakdown of Q.E.D.

CHAPTER III

RADIATIVE CORRECTIONS FOR PROCESSES OCCURRING IN e^+e^- COLLIDING BEAM EXPERIMENTS

III.1. Summary.

The methods used to calculate radiative corrections to the processes (II-1)-(II-3) are the same for the three cases. For this reason we will treat the case of muon pair production in full detail (because here the method is most easily demonstrated), whereas for the other reactions only the numerical results will be given [10].

As was indicated (chapter II) the calculation of radiative corrections involves the evaluation of the interference terms between the order α^2 term and the lowest order term (order α) in the scattering amplitude. The contributions of these terms to the cross section will be denoted by $d\sigma'/d\Omega$. In the following we will call these the virtual corrections. Furthermore when dealing with the bremsstrahlung correction an integral over photon phase space has to be considered.

First we will derive expressions for the virtual corrections; then we will treat the external photons in the soft photon approximation and demonstrate the cancellation of infrared divergences; finally the external photons will be treated without approximation.

In all calculations we assume that the incoming electrons and positrons are not polarized and also that the polarization of the outgoing particles is not detected.

III.2. Kinematics and the lowest order amplitude for $e^+e^- \rightarrow \mu^+\mu^-$.

We will consider the reaction

$$e^+(p_+) + e^-(p_-) \rightarrow \mu^+(q_+) + \mu^-(q_-). \quad (1)$$

The vectors in brackets are the four-momenta of the particles on the mass shell i.e.

$$\begin{aligned} p_{\pm}^2 &= m^2, & p_{\pm 0} &> 0, \\ q_{\pm}^2 &= \mu^2, & q_{\pm 0} &> 0. \end{aligned} \quad (2)$$

In these expressions m and μ are the electron and muon mass respectively^{*}. We choose the center of mass coordinate frame such that \vec{p}_+ is in the positive z -direction and \vec{q}_{\pm} are in the x - z plane. The scattering angle θ is the angle between \vec{p}_+ and \vec{q}_+ , E is the beam energy. From the momenta in (1) we construct the Mandelstam invariants

$$\begin{aligned} s &= (p_+ + p_-)^2 = (q_+ + q_-)^2, \\ t &= (q_+ - p_+)^2 = (q_- - p_-)^2, \\ u &= (q_- - p_+)^2 = (q_+ - p_-)^2. \end{aligned} \quad (3)$$

Due to the energy-momentum conservation these variables fulfil,

$$s + t + u = 2m^2 + 2\mu^2. \quad (4)$$

If we express these variables in terms of θ and E we get

$$\begin{aligned} s &= 4E^2, \\ t &= -(2E^2 - m^2 - \mu^2 - 2(E^2 - m^2)^{\frac{1}{2}}(E^2 - \mu^2)^{\frac{1}{2}}\cos\theta), \\ u &= -(2E^2 - m^2 - \mu^2 + 2(E^2 - m^2)^{\frac{1}{2}}(E^2 - \mu^2)^{\frac{1}{2}}\cos\theta). \end{aligned} \quad (5)$$

The three-momenta of the particles are given by

$$|\vec{p}_{\pm}| = (E^2 - m^2)^{\frac{1}{2}}, \quad |\vec{q}_{\pm}| = (E^2 - \mu^2)^{\frac{1}{2}}. \quad (6)$$

After these kinematical preliminaries we turn to the scattering amplitude. In lowest (non-trivial) order the amplitude for reaction (1) reads:

$$M = i(4\pi\alpha/s)\bar{u}(q_-)\gamma_{\mu}v(q_+)\bar{v}(p_+)\gamma^{\mu}u(p_-) = i(4\pi\alpha/s)T_0, \quad (7)$$

^{*}) Numerically we have:

$$m = 0.5110041(16) \text{ MeV}$$

$$\mu = 105.6595(3) \text{ MeV [11].}$$

corresponding to the diagram in fig. 3. In this formula α is the fine structure constant^{*}).

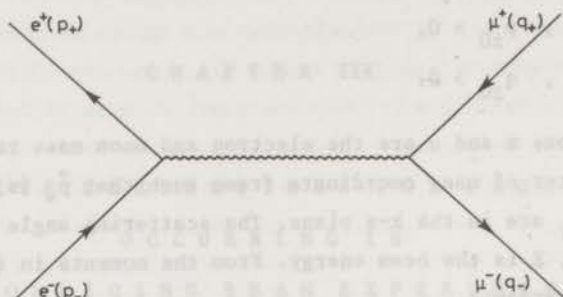


Fig. 3 Lowest order Feynman diagram for μ pair production.

Using formula (A.18) we can write the corresponding differential cross section as

$$\frac{d\sigma^0}{d\Omega_+} = \frac{1}{16\pi^2 s} \frac{|\vec{q}_+|}{|\vec{p}_+|} \cdot m^2 \mu^2 \sum_{\text{spins}} |M|^2. \quad (8)$$

In order to calculate this we need

$$X_0 = m^2 \mu^2 \sum_{\text{spins}} |T_0|^2 = \frac{1}{4}s^2 + 4\tau^2 + s(m^2 + \mu^2), \quad (9)$$

where we introduced the variable

$$\tau = \vec{p}_+ \cdot \vec{q}_+ = |\vec{p}_+| \cdot |\vec{q}_+| \cos \theta. \quad (10)$$

Using this intermediate result we obtain

$$\frac{d\sigma^0}{d\Omega_+} = \frac{\alpha^2}{2s} \frac{|\vec{q}_+|}{|\vec{p}_+|} \cdot \left[\frac{1}{2}(1 + \cos^2 \theta) + \frac{2(m^2 + \mu^2)}{s} (1 - \cos^2 \theta) + \frac{8m^2 \mu^2}{s^2} \cos^2 \theta \right].^{**} \quad (11)$$

In the relativistic limit, i.e. $s \gg m^2$ expression (11) reduces to

^{*}) Numerically: $\alpha = 1/137.03602(21)$ [11].

^{**}) Expression (11) has dimension (energy)⁻². In order to calculate the cross section in cm² one has to use the following conversion factor: $\hbar c = 1.9732891(66) \times 10^{-11}$ MeV cm [11].

expression (II.6).

The order α^2 contributions to the amplitude arise from the vertex corrections (figs. 4a-4b), the vacuum polarization (figs. 4c-4d) and the two-photon exchange graphs (figs. 4e-4f). Since we are interested in the cross section to order α^3 , we have to take into account the interference terms of the amplitudes $M^a - M^b$, (corresponding to figs. (4a)-(4f) with the basic amplitude M .

III.3 The vertex corrections.

The matrix elements M^a and M^b can be found using the Feynman rules of appendix A and are given by

$$M^a = \left(\frac{\alpha}{\pi}\right)^2 \frac{1}{s} \int d^4k \frac{\bar{u}(q_-) \gamma_\mu v(q_+) \bar{v}(p_+) \gamma_\alpha (-\not{p}_+ + \not{k} + m) \gamma^\mu (\not{p}_- + \not{k} + m) \gamma^\alpha u(p_-)}{(p_+) (p_-) (k)} \quad (12)$$

$$M^b = \left(\frac{\alpha}{\pi}\right)^2 \frac{1}{s} \int d^4k \frac{\bar{u}(q_-) \gamma_\alpha (\not{q}_- + \not{k} + \mu) \gamma_\mu (-\not{q}_+ + \not{k} + \mu) \gamma^\alpha v(q_+) \bar{v}(p_+) \gamma^\mu u(p_-)}{(q_+) (q_-) (k)} \quad (12')$$

where we have introduced the symbols:

$$\begin{aligned} (p_\pm) &= k^2 \mp 2(kp_\pm) + i\epsilon, \\ (q_\pm) &= k^2 \mp 2(kq_\pm) + i\epsilon, \\ (k) &= k^2 - \lambda^2 + i\epsilon, \end{aligned} \quad (13)$$

here λ is a small fictitious photon mass, introduced to regularize the infrared divergence. The contribution of these amplitudes to the cross section is given by

$$\frac{d\sigma^{a,b}}{d\Omega_+} = \frac{1}{16\pi^2 s} \frac{|\vec{q}_+|}{|\vec{p}_+|} m^2 \mu^2 \sum_{\text{spins}} 2\text{Re}(M^* M^{a,b}), \quad (14)$$

the star indicates complex conjugation.

Using the fact that the trace of a product of γ -matrices equals the trace of the product in reversed order it can easily be seen that the contribution of diagram 4b can be obtained by substituting $(m, p_\pm) \leftrightarrow (\mu, q_\pm)$ in the expression for $\sum 2\text{Re}(M^* M^a)$. It thus suffices to calculate $d\sigma^a/d\Omega_+$.

We now write M^a in the following way

$$M^a = i(4\pi\alpha/s) \bar{u}(q_-) \gamma_\mu v(q_+) \bar{v}(p_+) \Gamma^\mu(p_+, p_-, m) u(p_-), \quad (15)$$

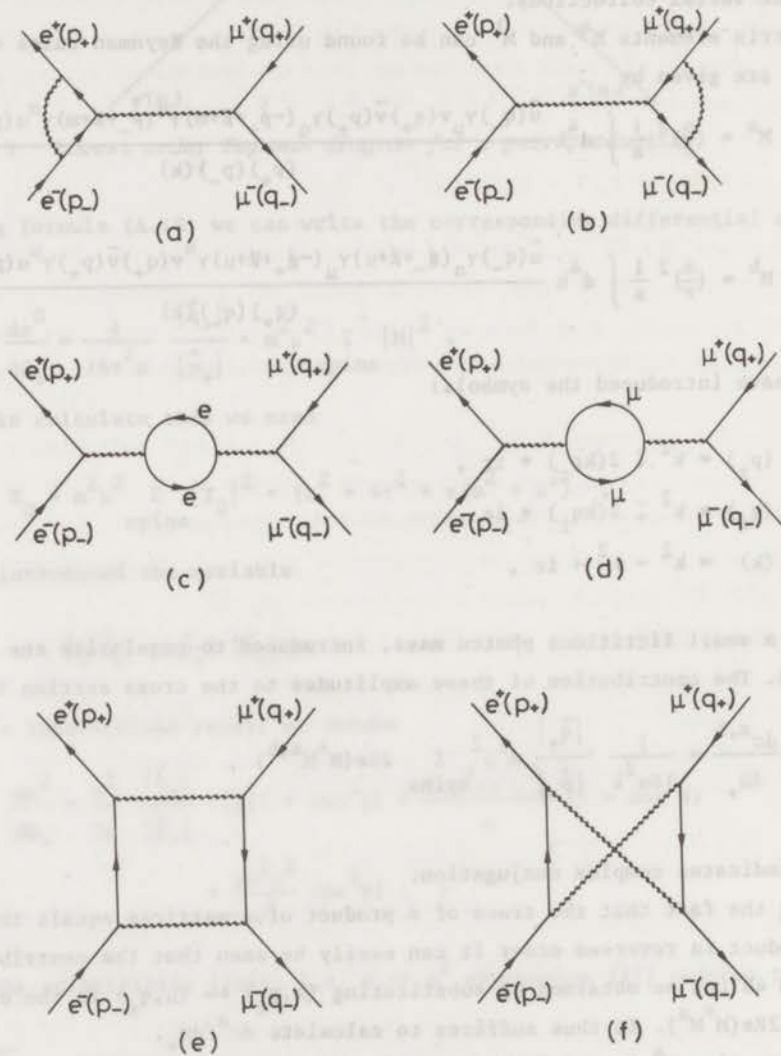


Fig. 4 Feynman diagrams for the virtual radiative corrections to μ pair production.

where

$$\Gamma^\mu = \frac{-i\alpha}{4\pi^3} \int d^4k \frac{\gamma_\alpha (-\not{p}_+ + \not{k} + m) \gamma^\mu (\not{p}_- + \not{k} + m) \gamma^\alpha}{(p_+)(p_-)(k)} \quad (16)$$

We proceed by splitting Γ^μ into three parts according to the number of times the vector k appears in the numerator of expression (15). We define

$$[I, I_\mu, I_{\mu\nu}] = \int d^4k \frac{[1, k_\mu, k_\mu k_\nu]}{(p_+)(p_-)(k)}, \quad (17)$$

and write the vertex function in the form

$$\Gamma^\mu = \frac{-i\alpha}{4\pi^3} (I M^\mu + I_\sigma M^{\mu\sigma} + I_{\sigma\rho} M^{\mu\sigma\rho}), \quad (18)$$

with

$$M^\mu = \gamma_\alpha (-\not{p}_+ + m) \gamma^\mu (\not{p}_- + m) \gamma^\alpha,$$

$$M^{\mu\sigma} = \gamma_\alpha [(-\not{p}_+ + m) \gamma^\mu \gamma^\sigma + \gamma^\sigma \gamma^\mu (\not{p}_- + m)] \gamma^\alpha, \quad (19)$$

$$M^{\mu\sigma\rho} = \gamma_\alpha \gamma^\sigma \gamma^\mu \gamma^\rho \gamma^\alpha.$$

The integrals (17) are calculated in appendix B, where we introduced an auxiliary variable ϕ . We find up to two terms of order λ ,

$$I = \frac{-2i\pi^2}{m \sin 2\phi} \left[\phi \log \frac{m}{\lambda} + \int_0^\phi \xi \operatorname{tg} \xi d\xi \right]. \quad (20)$$

The integral I_μ can be written as $I_\mu = I_\Delta \Delta_\mu$, with

$$I_\Delta = \frac{-2i\pi^2 \phi}{m^2 \sin 2\phi}, \quad (21)$$

where we introduced $\Delta = (p_+ - p_-)/2$. The integral $I_{\mu\nu}$ is decomposed in the following way.

$$I_{\mu\nu} = I_0 g_{\mu\nu} + I'_\Delta \Delta_\mu \Delta_\nu + I_P P_\mu P_\nu, \quad (22)$$

where $P = (p_+ + p_-)/2$. The coefficients are given by

$$I_0 = \frac{1}{4} \left[I_\infty - \frac{i\pi^2}{2} + 2i\pi^2 (1 - \phi \cot \phi) \right],$$

$$I'_\Delta = \frac{-i\pi^2 \phi}{m^2 \sin 2\phi} = \frac{1}{2} I_\Delta, \quad (23)$$

$$I_P = \frac{-i\pi^2}{2m^2 \sin^2 \phi} (1 - \phi \cotg \phi). \quad (23)$$

Here I_∞ is a divergent constant, to be disposed of by charge renormalization. For the matrices M in expression (18) we find

$$\begin{aligned} \bar{v}(p_+) M^\mu u(p_-) &= -4(p_+ p_-) \bar{v}(p_+) \gamma^\mu u(p_-), \\ \bar{v}(p_+) M^{\mu\sigma} \Delta_\sigma u(p_-) &= 4(p_+ p_-) \bar{v}(p_+) \gamma^\mu u(p_-) - 2m \bar{v}(p_+) [\gamma^\mu, \not{p}] u(p_-), \\ \bar{v}(p_+) M^{\mu\sigma\rho} g_{\sigma\rho} u(p_-) &= 4\bar{v}(p_+) \gamma^\mu u(p_-), \\ \bar{v}(p_+) M^{\mu\sigma\rho} \Delta_\sigma \Delta_\rho u(p_-) &= -((p_+ p_-) + 3m^2) \bar{v}(p_+) \gamma^\mu u(p_-) + 2m \bar{v}(p_+) [\gamma^\mu, \not{p}] u(p_-), \\ \bar{v}(p_+) M^{\mu\sigma\rho} p_\sigma p_\rho u(p_-) &= ((p_+ p_-) + m^2) \bar{v}(p_+) \gamma^\mu u(p_-). \end{aligned} \quad (24)$$

We see that we can write

$$\bar{v}(p_+) \Gamma^\mu u(p_-) = \bar{v}(p_+) \{ \gamma^\mu F_1 + \frac{1}{4m} [\gamma^\mu, \not{p}_+ + \not{p}_-] F_2 \} u(p_-), \quad (25)$$

here F_1 and F_2 are functions of m^2 and ϕ or of m^2 and s . Now F_1 is divergent because it contains I_∞ via I_0 . By subtracting from $F_1(s, m^2)$ its value at $s = 0$ (which is equivalent to $\phi = 0$) we can perform a charge renormalization. If we look at $M + M^a$ we see that we can transfer this $F_1(0, m^2)$ from M^a to M and absorb it in the electron charge [3]. We will now call the difference $F_1 - F_1(0)$, F_1 .

In terms of ϕ we find for $F_{1,2}$

$$\begin{aligned} F_1 &= -\frac{\alpha}{\pi} \frac{2}{\text{tg} 2\phi} \{ \phi (\log \frac{m}{\lambda} - 1) + \int_0^\phi \xi \text{tg} \xi d\xi \} + \frac{\alpha}{\pi} \log \frac{m}{\lambda} \\ &\quad - \frac{\alpha}{\pi} + \frac{\alpha}{2\pi} \phi \text{tg} \phi, \end{aligned} \quad (26)$$

$$F_2 = \frac{\alpha}{\pi} \frac{\phi}{\sin 2\phi}$$

For physical values of s , (i.e. $s > 4m^2$), we have

$$\phi(s) = \frac{1}{2} \{ \pi - i \log b \}, \quad (27)$$

with

$$b = \frac{1-a}{1+a}, \quad a = (1 - 4m^2/s)^{\frac{1}{2}}. \quad (28)$$

These results for the vertex correction can be summarized in the following way. We get the expression for M^a if we replace the electron vertex γ^μ in (6) by

$$\gamma^\mu F_1(s, m^2) + \frac{1}{4m} [\gamma^\mu, \not{p}_+ + \not{p}_-] F_2(s, m^2). \quad (29)$$

From (14), (15) and (16) it can be seen that we only need the real parts of $F_{1,2}$. Using the expression (27) for $\phi(s)$, those are given by

$$\begin{aligned} \text{Re}F_1(s, m^2) = & -\frac{\alpha}{\pi} \left\{ 1 + \frac{1 + 2a^2}{2a} \log b + \right. \\ & \left. \frac{1 + a^2}{2a} \left[-\text{Li}_2(b) - \frac{1}{3} \pi^2 + \frac{1}{4} (\log b)^2 - \log b \log(1-b) \right] - \right. \end{aligned} \quad (30)$$

$$\left. \left(1 + \frac{1 + a^2}{2a} \log b \right) \log \frac{m}{\lambda} \right\},$$

$$\text{Re}F_2(s, m^2) = \frac{\alpha}{\pi} \frac{(1 - a^2)}{4a} \log b. \quad (31)$$

With the help of these functions we can write

$$\frac{d\sigma^a}{d\Omega_+} = \frac{d\sigma^0}{d\Omega_+} \cdot 2\text{Re}F_1(s, m^2) + \frac{d\sigma^{a, \text{mag}}}{d\Omega_+} (m^2), \quad (32)$$

where

$$\frac{d\sigma^{a, \text{mag}}}{d\Omega_+} (m^2) = \frac{\alpha^2}{s} \frac{|\vec{q}_+|}{|\vec{p}_+|} \left(1 + \frac{2\mu^2}{s} \right) \text{Re}F_2(s, m^2). \quad (33)$$

With these expressions and the substitution rule for the contribution of M^b the vertex correction is given. (The index mag is used in (32) and (33) because the term $d\sigma^{a, \text{mag}}/d\Omega_+$ is due to the anomalous magnetic moment of the electron.)

III.4. Vacuum polarization corrections.

In the treatment of vacuum polarization we will only calculate the effect due to electrons and muons. We will ignore the contributions of hadronic intermediate states for the following reason.

Hadronic vacuum polarization is not an effect which can be calculated from field theory alone. The usual approach to obtain numerical corrections is the use of dispersion relations, using as input the total cross section for $e^+e^- \rightarrow \text{hadrons}$, as a function of energy. However in doing so, new assumptions beyond Q.E.D. have to be made.*)

*) The assumption that the vacuum polarization tensor obeys a dispersion relation has been tested experimentally in the region of the ϕ resonance and was proven to be correct [12].

In case the center of mass energy is greater than 1 GeV, the cross section is increased by $\pm 1\%$ (independent of energy) ^{**}.

We now turn to the calculation of the amplitudes M^c and M^d . These are given by

$$M^c = \left(\frac{\alpha}{\pi}\right)^2 \frac{1}{s} \int d^4k \frac{\bar{u}(q_-) \gamma_\mu v(q_+) \text{Tr}[\gamma^\mu (\not{P} + \not{k} + m) \gamma^\nu (-\not{P} + \not{k} + m)] \bar{v}(p_+) \gamma^\nu u(p_-)}{(m_+)(m_-)} \quad (34)$$

$$M^d = \left(\frac{\alpha}{\pi}\right)^2 \frac{1}{s} \int d^4k \frac{\bar{u}(q_-) \gamma_\mu v(q_+) \text{Tr}[\gamma^\mu (\not{P} + \not{k} + \mu) \gamma^\nu (-\not{P} + \not{k} + \mu)] \bar{v}(p_+) \gamma^\nu u(p_-)}{(\mu_+)(\mu_-)} \quad (35)$$

where we introduced

$$(m_\pm) = (k \pm P)^2 - m^2 + i\epsilon, \quad (36)$$

$$(\mu_\pm) = (k \pm P)^2 - \mu^2 + i\epsilon.$$

In appendix B is shown that (after charge renormalization) M^c can be written as

$$M^c = -M \cdot \Pi(s, m^2) \quad (37)$$

We obtain M^d if in the expression for Π we make the substitution $m \rightarrow \mu$. The real part of Π is given by

$$\text{Re } \Pi(s, m^2) = \frac{\alpha}{\pi} \left[\frac{8}{9} - \frac{a^2}{3} + a \left(\frac{1}{2} - \frac{a^2}{6} \right) \log b \right], \quad (38)$$

where definition (28) of a and b is used. The correction due to vacuum polarization can be summarized as

**) Relevant formulae and the experimental inputs for this estimate can be found in [21].

***) The expression for $\text{Re } \Pi(s, m^2)$ given in [10] contains the following misprint. The coefficient of $\log b$ is given as $\left(\frac{1}{2} - \frac{a^2}{3}\right)$ instead of $\left(\frac{1}{2} - \frac{a^2}{6}\right)$.

$$\frac{d\sigma^f}{d\Omega_+}(s,t) = -\frac{d\sigma^e}{d\Omega_+}(s,u) \quad (43)$$

It thus suffices to calculate M^e .

We proceed by splitting M^e in three parts according to the number of times the vector k appears in the numerator. We define

$$[J; J_\mu; J_{\mu\nu}] = \int d^4k \frac{[1; k_\mu; k_\mu k_\nu]}{(\Delta)(Q)(+)(-)} \quad (44)$$

and write the matrix element M^e in the form

$$M^e = \left(\frac{\alpha}{\pi}\right)^2 (JT + J^\mu T_\mu + J^{\mu\nu} T_{\mu\nu}) \quad (45)$$

A straightforward trace calculation provides us with the quantities

$$[X; X_\mu; X_{\mu\nu}] = m^2 \mu^2 \sum_{\text{spins}} T_0^* [T; T_\mu; T_{\mu\nu}] \quad (46)$$

and we have

$$\frac{d\sigma^e}{d\Omega_+} = \frac{\alpha^3}{\pi} \frac{1}{s^2} \frac{|\vec{q}_+|}{|\vec{p}_+|} \frac{1}{2\pi^2} \text{Im}(XJ + X_\mu J^\mu + X_{\mu\nu} J^{\mu\nu}) \quad (47)$$

The integral J is infrared divergent. It is convenient to write it as a sum of two terms

$$J = (F + G)/2P^2, \quad (48)$$

where

$$F = \int d^4k (P^2 - k^2) / (\Delta)(Q)(+)(-), \quad (49)$$

$$G = \int d^4k / (\Delta)(Q)(+).$$

Of these integrals only G is infrared divergent. To write J as in eq. (48) we have made use of the fact that J_μ can be written as

$$J_\mu = J_\Delta \Delta_\mu + J_Q Q_\mu, \quad (50)$$

without a term proportional to P_μ . Multiplying eq. (50) with Δ_μ and Q_μ , and

solving for J_Δ and J_Q , we find

$$\begin{aligned} J_\Delta &= [\tau(F_\Delta + F) - Q^2(F_Q + F)]/2\Lambda, \\ J_Q &= [\tau(F_Q + F) - \Delta^2(F_\Delta + F)]/2\Lambda, \end{aligned} \quad (51)$$

where we have introduced $\Lambda = \Delta^2 Q^2 - \tau^2$, and

$$F_{\Delta,Q} = \int d^4 k / (\Delta, Q) (+) (-). \quad (52)$$

Similarly, for $J_{\mu\nu}$ we write down the decomposition

$$J_{\mu\nu} = K_0 g_{\mu\nu} + K_P P_\mu P_\nu + K_\Delta \Delta_\mu \Delta_\nu + K_Q Q_\mu Q_\nu + K_X (Q_\mu \Delta_\nu + \Delta_\mu Q_\nu). \quad (53)$$

Also in this case terms linear in P_μ are absent. We can again solve for the coefficients of the tensors and find

$$\begin{aligned} K_0 &= \frac{1}{2}(F - G + H_P + H_\Delta + H_Q) + P^2(J_\Delta + J_Q), \\ K_P &= (F - G + 2H_P + H_\Delta + H_Q)/2P^2 - (J_\Delta + J_Q), \\ K_\Delta &= [Q^2(\frac{1}{2}H_\Delta - P^2 J_\Delta - K_0) - \tau(\frac{1}{2}H_\Delta - P^2 J_\Delta - \frac{1}{2}G_\Delta)]/\Lambda, \\ K_Q &= [\Delta^2(\frac{1}{2}H_Q - P^2 J_Q - K_0) - \tau(\frac{1}{2}H_Q - P^2 J_Q - \frac{1}{2}G_Q)]/\Lambda, \\ K_X &= [\Delta^2(\frac{1}{2}H_\Delta - P^2 J_\Delta - \frac{1}{2}G_\Delta) - (\frac{1}{2}H_\Delta - P^2 J_\Delta - K_0)]/\Lambda. \end{aligned} \quad (54)$$

To obtain $J_{\mu\nu}$ we have therefore to calculate the following simpler integrals:

$$\begin{aligned} H_\mu &= \int d^4 k k_\mu / (\Delta)(Q) (-) = H_P P_\mu + H_\Delta \Delta_\mu + H_Q Q_\mu, \\ G_{\Delta\mu} &= \int d^4 k k_\mu / (\Delta)(+) (-) = G_\Delta \Delta_\mu, \\ G_{Q\mu} &= \int d^4 k k_\mu / (Q)(+) (-) = G_Q Q_\mu. \end{aligned} \quad (55)$$

The analytic expressions for the integrals F , G , H_P , $H_{\Delta,Q}$ and $G_{\Delta,Q}$ are given in appendix B. It follows from these expressions that

$$-G + H_P + H_\Delta + H_Q = 0 \quad , \quad (56)$$

and consequently that K_0 and K_P can be simplified to

$$\begin{aligned} K_0 &= -\frac{1}{2}F + P^2(J_\Delta + J_Q) \quad , \\ K_P &= (\frac{1}{2}H_P - K_0)/P^2 \quad . \end{aligned} \quad (57)$$

The last step in the process of calculating $d\sigma^e/d\Omega_+$ is now to contract X_μ and $X_{\mu\nu}$ with the different tensors of the decomposition of J_μ and $J_{\mu\nu}$:

$$\begin{aligned} X &= (4\tau + \frac{1}{2}s)X_0 - s^2\tau \quad , \\ X_\mu \Delta^\mu &= -(2\Delta^2 + 4\tau)X_0 - 2s\tau^2 + (2s^2 + 8m^2\mu^2)\tau + 2s\Delta^2(\mu^2 + \frac{1}{2}s) \quad , \\ X_\mu Q^\mu &= -(2Q^2 + 4\tau)X_0 - 2s\tau^2 + (2s^2 + 8m^2\mu^2)\tau + 2sQ^2(m^2 + \frac{1}{2}s) \quad , \\ X_{\mu\nu} g_{\mu\nu} &= 10X_0 + 12s\tau \quad , \\ X_{\mu\nu} P^\mu P^\nu &= \frac{1}{2}s(X_0 + 2s\tau) \quad , \\ X_{\mu\nu} \Delta^\mu \Delta^\nu &= 2\Delta^2 X_0 + 8m^2\tau^2 + 4s\Delta^2 + 2m^2\Delta^2 s \quad , \\ X_{\mu\nu} Q^\mu Q^\nu &= 2Q^2 X_0 + 8\mu^2\tau^2 + 4sQ^2\tau + 2\mu^2Q^2 s \quad , \\ X_{\mu\nu} (Q^\mu \Delta^\nu + \Delta^\mu Q^\nu) &= 6\tau X_0 + 6s\tau^2 + 8(m^2\mu^2 - s^2)\tau + 2s\Delta^2 Q^2 \quad . \end{aligned} \quad (58)$$

We now isolate the infrared divergent part of $d\sigma^e/d\Omega_+$. Notice that G is infrared divergent and that the infrared divergence of H_P can be identified with G . All other integrals being convergent, we have for the divergent piece of $d\sigma^e/d\Omega_+$:

$$\left(\frac{d\sigma^e}{d\Omega_+}\right)_\lambda = \frac{2\alpha^3}{\pi} \frac{|\vec{q}_+|}{|\vec{p}_+|} \frac{4\tau + s}{s^3} X_0 \frac{1}{2\pi^2} \text{Im } G \quad . \quad (59)$$

Note finally that with the definition (8) of X_0 the lowest order cross section derived from the Feynman diagram of fig. 3 can be written as

$$\begin{aligned}
 (42) \quad \frac{d\sigma^c}{d\Omega_+} &= \frac{d\sigma^0}{d\Omega_+} \cdot -2\text{Re} \Pi(s, m^2) \quad , \\
 \frac{d\sigma^d}{d\Omega_+} &= \frac{d\sigma^0}{d\Omega_+} \cdot -2\text{Re} \Pi(s, \mu^2) \quad .
 \end{aligned}
 \tag{39}$$

We defined $d\sigma^{c,d}/d\Omega_+$ in the same way as $d\sigma^{a,b}/d\Omega_+$ by means of eq. (13).

III.5. The two photon exchange contributions.

We now turn to the box diagrams, figs. (4e-4f). Applying the Feynman rules we get

$$\begin{aligned}
 M^e &= \left(\frac{\alpha}{\pi}\right)^2 \int d^4k \frac{\bar{u}(q_-) \gamma_\alpha (k - Q + \mu) \gamma_\beta v(q_+) \bar{v}(p_+) \gamma^\beta (k - A + m) \gamma^\alpha u(p_-)}{(\Delta)(Q)(+)(-)} \\
 M^f &= \left(\frac{\alpha}{\pi}\right)^2 \int d^4k \frac{\bar{u}(q_-) \gamma_\beta (-k - Q + \mu) \gamma_\alpha v(q_+) \bar{v}(p_+) \gamma^\beta (k - A + m) \gamma^\alpha u(p_-)}{(\Delta)(Q')(+)(-)}
 \end{aligned}
 \tag{40}$$

We have introduced the following symbols

$$\begin{aligned}
 (\Delta) &= k^2 - 2(kA) - P^2 + i\epsilon \quad , \\
 (Q) &= k^2 - 2(kQ) - P^2 + i\epsilon \quad , \\
 (Q') &= k^2 + 2(kQ') - P^2 + i\epsilon \quad , \\
 (\pm) &= k^2 \pm 2(kP) + P^2 - \lambda^2 + i\epsilon \quad ,
 \end{aligned}
 \tag{41}$$

where $Q = \frac{1}{2}(q_+ - q_-)$ and λ is a small fictitious photon mass, introduced to regularize the infrared divergence. The contribution of these amplitudes to the cross section is given by

$$\frac{d\sigma^{e,f}}{d\Omega_+} = \frac{1}{16\pi^2 s} \frac{|\vec{q}_+|}{|\vec{p}_+|} m_\mu^2 \sum_{\text{spins}} 2\text{Re}(M^* M^{e,f}) \quad .
 \tag{42}$$

It can easily be seen that the contribution of diagram 4f can be obtained by substituting $(Q, \mu) \rightarrow (-Q, \mu)$ in the expression for $d\sigma^e/d\Omega_+$ and by adding an overall minus sign. Note that in the final expressions only even powers of the masses appear. If the final result is expressed in terms of the Mandelstam variables this is tantamount to

$$\frac{d\sigma^0}{d\Omega_+} = \frac{\alpha^2}{s^3} \frac{|\vec{q}_+|}{|\vec{p}_+|} X_0 \quad (60)$$

It follows that

$$\left(\frac{d\sigma^e}{d\Omega_+}\right)_\lambda = \frac{d\sigma^0}{d\Omega_+} \frac{2\alpha}{\pi} (4\tau + s) \frac{1}{2\pi^2} \text{Im } G \quad (61)$$

In appendix B we show that $\text{Im } G$ can be rewritten in such a way that eq. (61) becomes

$$\left(\frac{d\sigma^e}{d\Omega_+}\right)_\lambda = -\frac{d\sigma^0}{d\Omega_+} \frac{\alpha}{2\pi} (4\tau + s) \left[A(s, t) \log\left(\frac{s}{\lambda^2}\right) + B(s, t) \right] \quad (62)$$

The total contribution of diagrams 5e and 5f becomes

$$\frac{d\sigma^{e+f}}{d\Omega_+} = \left[\left(\frac{d\sigma^e}{d\Omega_+}\right)_\lambda + \left(\frac{d\sigma^e}{d\Omega_+}\right)_{\text{fin.}} - (t \leftrightarrow u) \right], \quad (63)$$

where $(d\sigma^e/d\Omega_+)_{\text{fin.}}$ is obtained from eq. (47) and subsequent formulae by omitting all integrals G and that part of H_p proportional to G .

In the limit $E \gg \mu, m$ and for $\sin \theta \gg \mu/E, m/E$ ($E = \frac{1}{2}\sqrt{s}$), our expressions for the two photon graphs reduce to those existing in the literature [13].

III.6. The inelastic reaction.

As was indicated in II.3 the infrared divergences occurring in the vertex correction III.3 and the two photon exchange contributions III.5 cancel against a similar divergence which arises from the cross section for the inelastic reaction

$$e^+(p_+) + e^-(p_-) \rightarrow \mu^+(q_+) + \mu^-(q_-) + \gamma(k) \quad (64)$$

For this reaction we will first establish the exact differential cross section. The cross section for reaction (64) will be obtained from the expression

$$d\sigma^B = \frac{\alpha^3}{2\pi^2 s^{\frac{1}{2}}} \frac{1}{|\vec{p}_+|} m^2 \mu^2 \sum_{\text{spins}} |M^B|^2 \delta^4(p_+ + p_- - q_+ - q_- - k) \frac{d^3 q_+}{q_{+0}} \frac{d^3 q_-}{q_{-0}} \frac{d^3 k}{k_0} \quad (65)$$

where

$$M^B = \sum_{i=1}^4 M_i^B = \sum_{i=1}^4 N_i / D_i \quad (66)$$

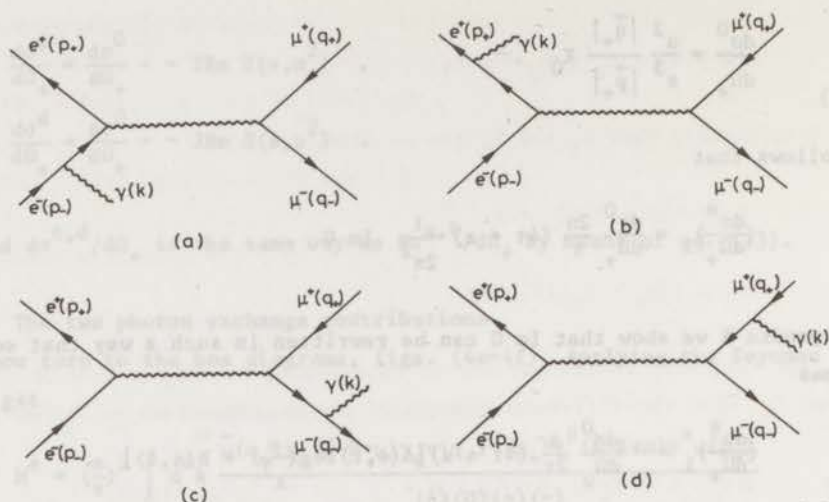


Fig. 5 Feynman diagrams for the production of a μ pair accompanied by real photon emission.

The four terms in M^B arise from the four diagrams of fig. 5. The denominators take the form

$$\begin{aligned} D_1 &= -2(kp_-)s', & D_2 &= -2(kp_+)s', \\ D_3 &= 2(kq_-)s, & D_4 &= 2(kq_+)s, \end{aligned} \quad (67)$$

with $s' = (q_+ + q_-)^2$.

The numerators consist of an electron and a muon part contracted with a photon polarization four vector, ϵ_α .

$$\begin{aligned} N_1 &= E^{\mu\alpha}(1)\epsilon_\alpha M_\mu(1), & N_2 &= E^{\mu\alpha}(2)\epsilon_\alpha M_\mu(2), \\ N_3 &= E_\mu(3)\epsilon_\alpha M^{\mu\alpha}(3), & N_4 &= E_\mu(4)\epsilon_\alpha M^{\mu\alpha}(4), \end{aligned} \quad (68)$$

with

$$\begin{aligned} E^{\mu\alpha}(1) &= \bar{v}(p_+)\gamma^\mu(\not{p}_- - \not{k} + m)\gamma^\alpha u(p_-), \\ E^{\mu\alpha}(2) &= \bar{v}(p_+)\gamma^\alpha(-\not{p}_+ + \not{k} + m)\gamma^\mu u(p_-), \\ E_\mu(3) &= E_\mu(4) = \bar{v}(p_+)\gamma_\mu u(p_-), \\ M_\mu(1) &= M_\mu(2) = \bar{u}(q_-)\gamma_\mu v(q_+), \\ M^{\mu\alpha}(3) &= \bar{u}(q_-)\gamma^\alpha(\not{q}_- + \not{k} + \mu)\gamma^\mu v(q_+), \end{aligned} \quad (69)$$

*) Because of the extra photon emitted it is no longer true that $(p_+ + p_-)^2 = (q_+ + q_-)^2$ as was the case with the virtual corrections.

$$M^{\mu\alpha}(4) = \bar{u}(q_-)\gamma^\mu(-\vec{q}_+ - \vec{k} + \nu)\gamma^\alpha v(q_+) \quad (69)$$

The quantity $\sum_{\text{spins}} |M^B|^2$ is now written in the form

$$\sum_{\text{spins}} |M^B|^2 = \frac{4}{\sum_{i,j=1}^4} \sum_{\text{spins}} \frac{N_i N_j}{D_i D_j} = \frac{4}{\sum_{i,j=1}^4} \frac{F_{ij}(p_+, p_-, q_+, q_-, k)}{D_i D_j} \quad (70)$$

The expressions for F_{ij} are given in appendix C.

From eq. (65), multi-differential cross sections are derived, and the question of the choice of integration variables now arises. Since we are primarily interested in the simulation of $e^+e^- \rightarrow \mu^+\mu^-$ by the emission of an extra photon, it is preferable to choose anyhow $d\Omega_+$, the solid angle of the μ^+ , as variable. For the other three variables, one could choose, e.g. q_{+0} , q_{-0} and ϕ , the energies of the μ^+ and μ^- , and the angle between the (\vec{p}_+, \vec{q}_+) and (\vec{q}_+, \vec{q}_-) plane. Since we want to integrate (numerically) over these three variables to find the simulated $e^+e^- \rightarrow \mu^+\mu^-$ events, it turns out that it is more practical to choose variables in which the places of rapid variation in the multi-differential cross section are easily located. The cross section peaks sharply whenever the photon is emitted parallel to the electron or positron direction (and, to a lesser extent, to the μ^+ or μ^- direction). So it is advantageous to use the angular variables of the photon. The polar and azimuthal photon angles, θ_Y and ϕ_Y , are taken with respect to a frame where \vec{q}_+ defines the z-axis, and $\vec{q}_+ \wedge \vec{p}_+$ the y-axis.

As third variable, $k = |\vec{k}|$ is used, which is convenient in order to exhibit the infrared divergence associated with $k \rightarrow 0$.

From eq. (65), we obtain

$$\frac{\partial \sigma^B}{\partial \Omega_+ \partial \Omega_Y \partial k} = \frac{\alpha^3}{2\pi^2 s} \frac{|\vec{q}_+|}{|\vec{p}_+|} \frac{k}{2p_{+0} - k + \frac{q_{+0}}{|\vec{q}_+|} k \cos \theta_Y} m^2 \mu^2 \frac{4}{\sum_{i,j=1}^4} \frac{F_{ij}}{D_i D_j} \quad (71)$$

The expression for this cross section takes a very simple form when one assumes that in the quantities N_i , the photon momentum can be neglected, and that the emission of a photon does not alter the momenta of the muons. This approximation is obviously good when the photons are sufficiently soft (soft photon approximation). In this case we find

$$(69) \quad \frac{\partial \sigma^S}{\partial \Omega_+ \partial \Omega_\gamma \partial k} = \frac{\alpha^3}{2\pi^2 s^3} \frac{|\vec{q}_+|}{|\vec{p}_+|} \frac{k^2}{2p_+ k_0} X_0 \cdot B, \quad (72)$$

where

$$(70) \quad B = - \left(\frac{p_-}{(kp_-)} - \frac{p_+}{(kp_+)} - \frac{q_-}{(kq_-)} + \frac{q_+}{(kq_+)} \right)^2, \quad (73)$$

the square is to be taken in the sense of a Lorentz inner product.

In the expansion for B two sets of terms can be distinguished. First we have:

$$B_S = - \left(\frac{p_-}{(kp_-)} - \frac{p_+}{(kp_+)} \right)^2 - \left(\frac{q_-}{(kq_-)} - \frac{q_+}{(kq_+)} \right)^2, \quad (74)$$

the remainder is

$$B_D = B - B_S^* \quad (75)$$

The contributions from B_S cancel the i.r. divergences in the vertex correction, whereas B_D just compensates the divergences in the two photon exchange graphs.

As with the virtual corrections we have given the photon a small mass λ such that now we have to distinguish between $k = |\vec{k}|$ and $k_0 = \sqrt{k^2 + \lambda^2}$.

In the following it will be useful to integrate the cross section for isotropic photon emission, from zero momentum up to a specific maximal photon momentum k_1 . For the term denoted with S we find

$$\frac{d\sigma^S}{d\Omega_+} = \int_0^{k_1} dk \int_{-1}^{+1} d(\cos \theta_\gamma) \int_0^{2\pi} d\phi_\gamma \frac{\partial \sigma^S}{\partial \Omega_+ \partial \Omega_\gamma \partial k} = \frac{d\sigma^0}{d\Omega_+} [\delta_S(m^2, k_1) + \delta_S(\mu^2, k_1)] \quad (76)$$

with

$$(77) \quad \delta_S(m^2, k_1) = - \frac{\alpha}{\pi} \left\{ \left[2 + \frac{1+a^2}{a} \log b \right] \log \frac{2k_1}{\lambda} + \frac{1}{a} \log b + \frac{1+a^2}{a} \left[\text{Li}_2 \left(\frac{2a}{1+a} \right) + \frac{1}{4} (\log b)^2 \right] \right\} \quad (77)$$

*) For the meaning of the subscripts S and D see sect. IV.1.

It can be seen from (30) and (32), that the sum of $d\sigma^a/d\Omega_+$, $d\sigma^b/d\Omega_+$ and $d\sigma^S/d\Omega_+$ no longer contains terms which diverge if $\lambda = 0$.

For $d\sigma_S^S/d\Omega_+$ defined in analogy with $d\sigma_S^S/d\Omega_+$ we find

$$\frac{d\sigma_D^S}{d\Omega_+} = \frac{d\sigma^0}{d\Omega_+} \cdot \delta_D(s, t), \quad (78)$$

with

$$\delta_D(s, t) = \frac{\alpha}{2\pi} \{ (4\tau + s) [A(s, t) \log(\frac{2k_1}{\lambda})^2 + C(s, t)] - (t \leftrightarrow u) \}. \quad (79)$$

For the details of these integrations we refer to appendix B. From eq. (62) it is explicitly seen that here also the λ dependence disappears.

We have thus seen that the infrared divergences disappear by taking into account inelastic processes as well as elastic ones.

III.7. Phase space and acoplanarity.

We will now derive formulae which can be used to translate certain experimental constraints in limits on the integration variables k , θ_γ and ϕ_γ (see eq. (76)).

A useful tool is the Dalitz plot for the three particles μ^+ , μ^- and γ . In a Dalitz plot the kinematical configuration of the outgoing particles is determined by three coordinates which are q_{+0} , q_{-0} and ϕ (see page 29).

These coordinates have the advantage that a volume element in phase space is directly proportional to $dq_{+0} dq_{-0} d\phi$ without a (q_{+0}, q_{-0}, ϕ) dependent factor.

Some often occurring conditions, like $\theta_\gamma = \text{constant}$, or $\delta = \text{constant}$, where δ is the angle between \vec{q}_+ and \vec{q}_- , represent curves in the Dalitz plot, i.e. they are relations between the variables q_{+0} and q_{-0} . (From now on we will not mention the ϕ dependence and concentrate on what happens for fixed ϕ in the q_{+0}, q_{-0} plane, which plane is the Dalitz plot.) A special case is the boundary of the Dalitz plot itself. These curves are obtained by using the four vector n^μ , defined as

$$n^\mu = 2\epsilon^{\mu\nu\rho\sigma} p_\nu q_{+\rho} q_{-\sigma}, \quad (80)$$

or

$$n^\mu = -2\epsilon^{\mu\nu\rho\sigma} P_\nu q_{+\rho} k_\sigma, \quad (81)$$

where $P = (p_+ + p_-)/2$ as was the case with the virtual corrections. In the c.m.s., only the spatial components are different from zero: they are proportional to the vector products $\vec{q}_+ \wedge \vec{q}_-$ or $\vec{q}_+ \wedge \vec{k}$, i.e. proportional to $\sin \delta$ or

$\sin \theta_Y$. So we find for n^2 , on the one hand

$$n^2 = -4P_0^2 |\vec{q}_+|^2 |\vec{q}_-|^2 \sin^2 \delta, \quad (82)$$

$$n^2 = -4P_0^2 |\vec{q}_+|^2 (P_0 - q_{+0} - q_{-0})^2 \sin^2 \theta_Y, \quad (83)$$

and on the other hand (from eq. (80)),

$$n^2 = -4 \begin{vmatrix} P^2 & (Pq_+) & (Pq_-) \\ (Pq_+) & \mu^2 & (q_+q_-) \\ (Pq_-) & (q_+q_-) & \mu^2 \end{vmatrix} = -4P_0^2 \begin{vmatrix} 1 & q_{+0} & q_{-0} \\ q_{+0} & \mu^2 & (q_+q_-) \\ q_{-0} & (q_+q_-) & \mu^2 \end{vmatrix}. \quad (84)$$

Combining (84) with either (82) or (83), and eliminating (q_+q_-) with

$$(q_+q_-) = -\mu^2 - 2P_0^2 + 2P_0(q_{+0} + q_{-0}), \quad (85)$$

we obtain the curves for fixed $\sin \delta$ or $\sin \theta_Y$.

The fixed $\sin \delta$ relation reads

$$(\eta q_{+0} + \rho)^2 = |\vec{q}_+|^2 |\vec{q}_-|^2 \cos^2 \delta, \quad (86)$$

where

$$\eta = q_{-0} - 2P_{-0}, \quad \rho = \frac{1}{2}(\eta^2 - q_{-0}^2 + 2\mu^2). \quad (87)$$

More explicitly, this leads to the curves

$$q_{+0} = \frac{-\eta\rho \pm \sqrt{D}}{\eta^2 - (q_{-0}^2 - \mu^2)\cos^2 \delta} \equiv B_{\pm}(q_{-0}, \cos^2 \delta), \quad (88)$$

with

$$D = |\vec{q}_-|^2 \cos^2 \delta (\rho^2 - \eta^2 \mu^2 + \mu^2 |\vec{q}_-|^2 \cos^2 \delta). \quad (89)$$

The upper sign corresponds to curve 1 in fig. 6, where $\cos \delta < 0$, and the lower sign to curves 2 ($\cos \delta < 0$) and 3 ($\cos \delta > 0$). The boundaries of the Dalitz plot are a special case:

$$q_{+0} = B_{\pm}(q_{-0}, 1) = \frac{1}{2}[-\eta \pm (|\vec{q}_-| - \frac{\mu^2}{\eta \mp |\vec{q}_-|})]. \quad (90)$$

The upper sign corresponds to curve I, where $\delta = \pi$ and $\theta_Y = \pi$, the lower sign

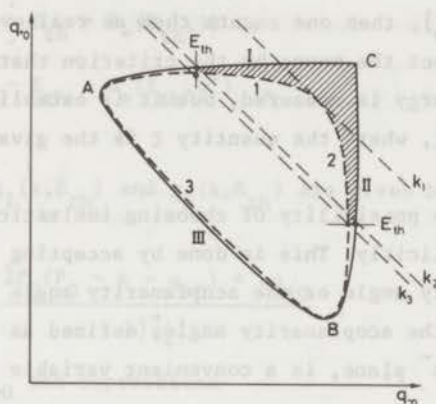


Fig. 6 Dalitz plot for the μ pair. The curves 1 and 2 are the lines where the muons make an angle $\pi - \zeta$. The shaded area is the experimental phase space.

to curves II and III, where $\delta = \pi$, $\theta_Y = 0$ and $\delta = 0$, $\theta_Y = \pi$ respectively. At the points A and B, $|\vec{q}_-|$ and $|\vec{q}_+|$ vanish.

In a similar fashion, using eqs. (83) and (84), fixed θ_Y curves are found.

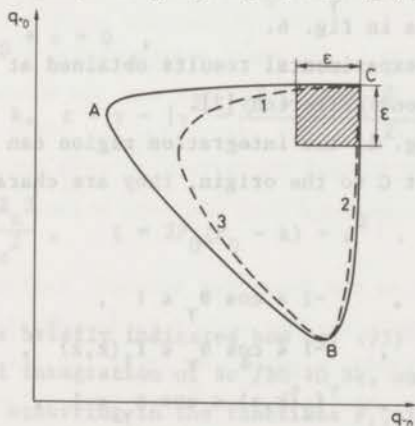


Fig. 7 Dalitz plot for the μ pair, showing the curves 1, 2 and 3, where $\theta_Y \approx \theta$ and $\theta_Y \approx \pi - \theta$.

In fig. 7 an example is drawn: along 1 and 3, $\cos \theta_Y < 0$, and along 2 $\cos \theta_Y > 0$.

Experimentally, when measuring the $e^+e^- \rightarrow \mu^+\mu^-$ reaction, one uses some criterion to decide whether the observed μ pairs belong to this reaction. We will consider two distinct possibilities.

In the first place, if the two muons are detected and their energies lie in the range $[p_{+0} - \varepsilon, p_{+0}]$, then one counts them as real events ^{*}). In the second place, one may select the muons by the criterion that they are produced back to back. Then, no energy is measured, but it is established that their tracks make an angle $\delta < \zeta$, where the quantity ζ is the given maximum acollinearity.

There exists also the possibility of choosing inelastic events only, i.e. to study reaction (4) explicitly. This is done by accepting only those events for which the acollinearity angle or the acoplanarity angle exceeds a certain minimum. Experimentally, the acoplanarity angle, defined as the angle between the μ^+e^+ plane and the μ^-e^- plane, is a convenient variable for displaying results.

Returning to the first case, one has to evaluate the influence of reaction (64) by integrating $\partial\sigma^B/\partial\Omega_+\partial\Omega_-\partial k$ over the shaded area of fig. 7 and over the full ϕ_γ range. In the second case, one has to integrate over an area in the phase space between the curves $\cos \delta = -1$ and $\cos \delta = \cos(\pi - \zeta) \equiv z$. Since there usually exists a threshold energy for the muons, E_{th} , below which they cannot be detected, the available phase space is further restricted by the conditions $q_{\pm 0} > E_{th}$. For every ϕ_γ , one then has to integrate the $\mu^+\mu^-\gamma$ cross section over the shaded area in fig. 6.

In chapter IV we give experimental results obtained at CEA. These data were analyzed using the second criterion [2].

As can be seen from fig. 6, the integration region can be divided into five areas. Going from point C to the origin, they are characterized by the following limits:

$$\begin{aligned}
 \text{(i)} \quad & 0 \leq k \leq k_1, \quad -1 \leq \cos \theta_\gamma \leq 1, \\
 \text{(ii)} \quad & k_1 \leq k \leq k_2, \quad -1 \leq \cos \theta_\gamma \leq f_1(k, z), \\
 \text{(iii)} \quad & k_1 \leq k \leq k_2, \quad f_2(k, z) \leq \cos \theta_\gamma \leq 1, \\
 \text{(iv)} \quad & k_2 \leq k \leq k_3, \quad g_1(k, E_{th}) \leq \cos \theta_\gamma \leq f_1(k, z), \\
 \text{(v)} \quad & k_2 \leq k \leq k_3, \quad f_2(k, z) \leq \cos \theta_\gamma \leq g_2(k, E_{th}).
 \end{aligned} \tag{91}$$

Here

$$k_1 = 2P_0 \left\{ -1 - z + 2 \left[(1+z) \left(\frac{1}{2} - \frac{\mu^2}{4P_0^2} (1-z) \right) \right]^{\frac{1}{2}} \right\} / (1-z), \tag{92}$$

^{*}) Notice that the energies of the muons can never exceed p_{+0} .

$$\begin{aligned}
 k_2 &= 2P_0 - E_{th} - B_+(E_{th}, 1) , \\
 k_3 &= 2P_0 - E_{th} - B_+(E_{th}, z^2) ,
 \end{aligned}
 \tag{92}$$

and the functions $g_1(k, E_{th})$ and $g_2(k, E_{th})$ are given by the right hand side of the equation

$$\cos \theta_Y = \frac{2P_0(P_0 - k - q_{+0}) + kq_{+0}}{k|q_{+0}|} ,
 \tag{93}$$

by inserting for q_{+0} the expressions

$$q_{+0} = 2P_0 - E_{th} - k , \quad q_{+0} = E_{th} ,
 \tag{94}$$

respectively.

The functions $f_1(k, z)$ and $f_2(k, z)$ are also obtained from eq. (93) by inserting the q_{+0} values corresponding to the intersections of a fixed k -line with the curves 1 and 2 of fig. 6. These two q_{+0} values are the roots of the equation

$$q_{+0}^2 - bq_{+0} + c = 0 ,
 \tag{95}$$

where

$$b = 2P_0 - k , \quad c = \gamma - \left[\gamma^2 - \frac{\xi^2 + z^2 \mu^2 (b^2 - \mu^2)}{1 - z^2} \right]^{\frac{1}{2}} .
 \tag{96}$$

with

$$\gamma = \frac{\xi + \mu^2 z^2}{1 - z^2} , \quad \xi = 2P_0(P_0 - k) - \mu^2 .
 \tag{97}$$

In appendix D, it is briefly indicated how eq. (95) is derived.

For the numerical integration of $\partial \sigma^B / \partial \Omega_+ \partial \Omega_Y \partial k$, one finally has to know all the scalar products occurring in the functions F_{ij} in terms of the variable k , $\cos \theta_Y$, and ϕ_Y . In order to obtain the scalar products in terms of these variables we use

$$q_{+0} = \frac{2bP_0(P_0 - k) - k \cos \theta_Y [4P_0^2(P_0 - k)^2 + \mu^2(k^2 \cos^2 \theta_Y - b^2)]^{\frac{1}{2}}}{b^2 - k^2 \cos^2 \theta_Y}
 \tag{98}$$

If we now want to integrate $\partial \sigma^B / \partial \Omega_+ \partial \Omega_Y \partial k$ as given by (71) over the region of phase space defined above, we will get the same divergence as in the soft

photon approximation. We avoid these problems by means of the following procedure. The region of phase space is divided in two parts; an isotropic part I, given by (91-i) and an anisotropic part AI, given by (91-ii)-(91-v). We now split the integration in the following way

$$\int_{I+AI} \frac{\partial \sigma^B}{\partial \Omega_+ \partial \Omega_Y \partial k} d\Omega_Y dk = \int_I \frac{\partial \sigma^S}{\partial \Omega_+ \partial \Omega_Y \partial k} d\Omega_Y \partial k + \int_I \frac{\partial (\sigma^B - \sigma^S)}{\partial \Omega_+ \partial \Omega_Y \partial k} + \int_{AI} \frac{\partial \sigma^B}{\partial \Omega_+ \partial \Omega_Y \partial k} . \quad (99)$$

The first integral was performed analytically (76)-(79). The second integral is convergent, because the singularity is subtracted out and finally the third integral is convergent as well.

The final results for $d\sigma/d\Omega_+$ can be written as follows

$$\frac{d\sigma}{d\Omega_+} = \frac{d\sigma^0}{d\Omega_+} (1 + \delta_A + \delta_N) = \frac{d\sigma^0}{d\Omega_+} (1 + \delta_T) . \quad (100)$$

A part of the total correction δ_T is known analytically, i.e. δ_A which corresponds to the sum of the virtual corrections and the correction due to the emission of a soft photon with maximal energy k_1 . The other part δ_N has to be evaluated numerically and represents the effect of hard anisotropic bremsstrahlung and the difference between hard and soft bremsstrahlung over an isotropic region.

The numerical integration was done over separate regions in phase space, chosen in such a way that small regions with a rapid variation of the integrand were attributed as many integration points as large regions with a small variation. Over every region, the integration was done using the multi-dimensional integration routine RIWIAD, which itself distributes the integration points as efficiently as possible over the integration domain [16].

Finally we turn to the study of reaction (64) looked upon as a lowest order process in its own right. One of the quantities which is most likely to be measured is the distribution of events as a function of the acoplanarity angle, ψ .

Let us introduce a new coordinate frame with \vec{p}_+ along the z-axis and $\vec{p}_+ \wedge \vec{q}_+$ along the y-axis. Then \vec{q}_+ has a polar angle θ and a vanishing azimuthal

angle. The corresponding quantities for q^- are θ' and ϕ' . When we have an elastic event, $\theta' = \pi - \theta$ and $\phi' = \pi$. Therefore, it is natural to define the acoplanarity angle by $\psi = \pi - \phi'$.

The above-mentioned acoplanarity distribution is then defined by

$$\frac{d\sigma}{d\psi} = \int \frac{\partial \sigma^B}{\partial \Omega_+ \partial \Omega_- \partial q_{-0}} d(\cos \theta') d\Omega_+ dq_{-0}, \quad (101)$$

where the integral has to be carried out over the phase space region determined by the experimental conditions:

$$\theta_{\min} \leq \theta, \theta' \leq \theta_{\max}, \quad (102)$$

$$q_{+0}, q_{-0} \geq E_{th}. \quad (103)$$

We assume that the detection of μ^+ and μ^- goes over the full azimuthal range, giving a factor 2π . If this is not the case, it is easy to make the necessary corrections.

Again, as the charge is undetected, we have to add $d\sigma(\psi)/d\psi$ and $d\sigma(2\pi - \psi)/d\psi$, giving twice expression (101).

The integrand in eq. (101) is given by

$$\frac{\partial \sigma^B}{\partial \Omega_+ \partial \Omega_- \partial q_{-0}} = \frac{\alpha^3}{4\pi^2} \frac{m^2 \mu^2}{2P_0 |\vec{p}_+|} \frac{|\vec{q}_+| |\vec{q}_-|}{2P_0 - q_{-0} + q_{+0} \frac{|\vec{q}_-|}{|\vec{q}_+|} \cos \delta} \sum_{i,j=1}^4 \frac{F_{ij}}{D_i D_j}. \quad (104)$$

Only the integration over q_{-0} deserves some explanation. Once θ' and ϕ' are given, $\cos \delta$ is fixed. The q_{-0} integration runs, when $\delta < \frac{1}{2}\pi$, over that part of line 3 in fig. 6 which is allowed by condition (103). Similarly, when $\delta > \frac{1}{2}\pi$, one has to integrate along the allowed portions of lines 1 and 2.

III.8. Bhabha scattering and two gamma production.

The virtual and soft photon corrections for Bhabha scattering were calculated by Redhead and Polovin [14]. The hard photon matrix element was calculated by Swanson [15]. The hard photon corrections to Bhabha scattering can be calculated in the same way as we presented for mu-pair production, making use of the above-mentioned work. The formulae for the phase space integration

CHAPTER IV

NUMERICAL RESULTS AND DISCUSSION

IV.1. Summary

We will present results on the three processes (II.1)-(II.3). In the first place we will look at the reaction $e^+e^- \rightarrow e^+e^-$ because recently experimental results have become available on this process. Then we will look at $e^+e^- \rightarrow \mu^+\mu^-$ where we distinguish two separate cases. First we assume that experimentally the charge of the outgoing muons is not detected. In this case the sum

$$S(\theta) = \frac{d\sigma(\theta)}{d\Omega} + \frac{d\sigma(\pi-\theta)}{d\Omega} \quad (1)$$

is measured. The amplitudes M^e and M^f of chapter III do not contribute to S . This is also the case for the inelastic contribution arising from interference between amplitudes where the electrons radiate and where the muons radiate. The function S defines (to order α^3) a correction δ_S which is defined by

$$S(\theta) = 2 \frac{d\sigma^0}{d\Omega_+} (1 + \delta_S) \quad (2)$$

The fact that for the function S , the two photon exchange graphs do not contribute is a consequence of a theorem by Potzulo [17].

If their charge is not measured the events will be selected according to the criterion that the muons have enough energy to trigger the detectors and that their traces are sufficiently collinear.

In case the charges are measured the full differential cross section is measured and all amplitudes contribute. Now also the energies of the muons will be known accurately so that here we apply the criterion that the energy loss of the muons does not exceed a fixed energy ε , i.e. $q_{\pm 0} > E - \varepsilon$.

Now we also define a function

$$D(\theta) = d\sigma(\theta)/d\Omega_+ - d\sigma(\pi - \theta)/d\Omega_+ \quad (3)$$

and a corresponding δ_D by

$$D(\theta) = 2 \frac{d\sigma^0}{d\Omega_+} \cdot \delta_D \quad (4)$$

Finally we will look at $e^+e^- \rightarrow \gamma\gamma$ a reaction which was studied by Berends and Gastmans [9].

For the three reactions we will give a table of the lowest order cross section at energies of 1,2,3 and 5 GeV per beam. Then tables will be given where the corrections are given for specific event selection criteria. Finally a table will be given for the acoplanarity distribution. Here one obtains information on the pure inelastic process, i.e. the basic process with one extra photon emitted.

IV.2. Bhabha scattering.

As the differential cross section for Bhabha scattering diverges in the forward direction, we only give the values of $d\sigma^0/d\Omega_+$ from $\theta = 5^\circ$.

Table 1

The lowest order cross section for Bhabha scattering (in nb) for different values of the beam energy, P_{+0} (in GeV), and the scattering angle, θ .

P_{+0} θ	1.0	2.0	3.0	5.0
5°	$1427 \cdot 10^3$	$3566 \cdot 10^2$	$1585 \cdot 10^2$	$5706 \cdot 10^1$
20°	5373	1343	597.0	214.9
40°	304.6	76.15	33.85	12.18
60°	54.75	13.69	6.08	2.19
90°	11.66	2.92	1.30	0.47
120°	6.08	1.52	0.68	0.24
140°	5.35	1.34	0.59	0.21
160°	5.19	1.30	0.58	0.21
175°	5.18	1.30	0.58	0.21

The order α^3 contributions are given as a correction δ_T such that the cross section to this order is given by $d\sigma^0/d\Omega_+ (1 + \delta_T)$. In table 2 the δ_T are given for the case that the acollinearity does not exceed 10° . Furthermore the minimum energy necessary to trigger the detection system is taken to be 0.2 GeV.*)

*.) The errors on the corrections are errors in the numerical integration.

Table 2

The radiative corrections (in %) to the lowest order cross section for Bhabha scattering for different values of the beam energy, p_{+0} (in GeV), and the scattering angle, θ . The acollinearity angle $\zeta = 10^\circ$, and the threshold energy $E_{th} = 0.2$ GeV.

$\theta \backslash p_{+0}$	1.0	2.0	3.0	5.0
5°	9.7 ± 0.6	22.2 ± 1.5	33.9 ± 3.6	46.1 ± 3.4
20°	1.2 ± 0.1	1.7 ± 0.1	2.0 ± 0.1	2.2 ± 0.1
40°	-3.6 ± 0.1	-3.6 ± 0.1	-3.8 ± 0.1	-3.9 ± 0.1
60°	-6.3 ± 0.1	-6.5 ± 0.1	-6.7 ± 0.1	-6.8 ± 0.1
90°	-8.3 ± 0.1	-8.6 ± 0.1	-8.8 ± 0.1	-9.0 ± 0.1
120°	-8.9 ± 0.1	-9.1 ± 0.1	-9.3 ± 0.1	-9.4 ± 0.1
140°	-8.7 ± 0.1	-8.7 ± 0.1	-8.7 ± 0.1	-8.8 ± 0.1
160°	-7.9 ± 0.1	-7.5 ± 0.1	-7.4 ± 0.1	-7.3 ± 0.1
175°	-7.3 ± 0.1	-5.9 ± 0.1	-5.7 ± 0.1	-4.5 ± 0.1

From table 2 we see that in the neighbourhood of $\theta = 5^\circ$ the corrections become large and positive. (This effect differs from the one mentioned in section II.5.) It can be understood as follows. If we look at the Coulomb scattering graph for $e^+e^- \rightarrow e^+e^-$ we see that emission of an extra photon in the region of small θ reduces the momentum transfer through the photon in the t -channel, thus increasing the amplitude (which behaves as t^{-1}). This enhances the inelastic amplitude which is large already if the extra photon is emitted parallel to one of the charged particles.

We will now give the acoplanarity distribution $d\sigma/d\psi$. Here we assume that the outgoing electrons and positrons are detected within the angular range $45^\circ \leq \theta_{\pm} \leq 135^\circ$. Here also the threshold energy is 0.2 GeV (table 3).

Recently experimental data have become available on Bhabha scattering. The experiments were performed at beam energies of 2.0 GeV and 2.5 GeV. The criteria for selecting events and the procedure of analyzing the data are described in [2]. The main features are, a maximum collinearity of 15° and a threshold energy of 0.8 GeV.

Table 3

The acoplanarity distribution, $d\sigma/d\psi$ for Bhabha scattering, for a beam energy of 2.0 GeV and for different acoplanarity angles ψ . The threshold energy

$$E_{th} = 0.2 \text{ GeV, and } \theta_{min} = 45^\circ, \theta_{max} = 135^\circ.$$

ψ	$\frac{d\sigma}{d\psi}$ (nb)
5°	9.32 ± 0.16
10°	2.99 ± 0.03
20°	0.86 ± 0.01
40°	0.22 ± 0.01
60°	0.10 ± 0.01
90°	0.05 ± 0.01
120°	0.03 ± 0.01
150°	0.03 ± 0.01
180°	8.46 ± 0.08

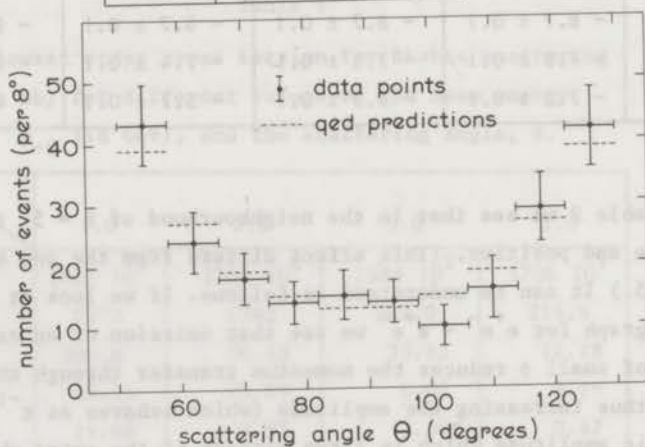


Fig. 8 Angular distribution of scattered particles in elastic e^+e^- scattering at the energy $2p_{+0} = 5$ GeV, and the prediction of QED normalized to the total number of observed events.

In fig. 8, the experimental and theoretical cross sections are given for a beam energy of 2.5 GeV. In order to compare experiment and theory both the experimental and theoretical cross sections are integrated over the θ range of the detection apparatus ($45^\circ \leq \theta \leq 135^\circ$) giving σ_{exp} and σ_{th}^* (For both

*.) Note that these σ 's are not total cross sections.

energies the order α^3 corrections were $-7.7 \pm 0.8\%$.) We now define the ratio $R = \sigma_{\text{exp}}/\sigma_{\text{th}}$. The analysis of the data yielded the following numbers for this ratio.

$$E = 2.0 \text{ GeV} \quad R = 0.93 \pm 0.10$$

$$E = 2.5 \text{ GeV} \quad R = 1.03 \pm 0.09$$

One can parametrize the breakdown of Q.E.D. if one multiplies the photon propagator by a factor $(1 \pm q^2/(q^2 - \Lambda_{\pm}^2))$. The results given correspond to the following lower limits on Λ_{\pm} . (90% conf. level.)

$$E = 2.0 \text{ GeV} \quad \Lambda_+ > 9.8 \text{ GeV}, \quad \Lambda_- > 10.5 \text{ GeV}$$

$$E = 2.5 \text{ GeV} \quad \Lambda_+ > 9.7 \text{ GeV}, \quad \Lambda_- > 4.7 \text{ GeV}$$

Using the conversion factor given in the footnote on page 16, one can give Λ_{\pm}^{-1} in cm. ($(10 \text{ GeV})^{-1} \approx 2.10^{-15} \text{ cm}$.) The results thus indicate that for distances greater than $\approx 2.10^{-15} \text{ cm}$ Q.E.D. gives an accurate description of nature. Besides the differential cross section for Bhabha scattering one has also measured the acoplanarity distribution (in integrated form). In this way theoretical predictions for the reaction $e^+e^- \rightarrow e^+e^-\gamma$ can be compared with experiment. Experimentally one defines

$$\eta_{\text{exp}}(\psi_{\text{min}}) = N(\psi)/N_{\text{tot}} \quad (5)$$

where $N(\psi)$ is the total number of events with $\psi > \psi_{\text{min}}$ and N_{tot} is the total number of $e^+e^- \rightarrow e^+e^-$ events. The theoretical counterpart $\eta_{\text{QED}}(\psi_{\text{min}})$ can be calculated if one integrates expression (III-101) over the indicated region. The results displayed in table 3a show excellent agreement between experiment and theory.

Table 3a
Noncoplanarity-angle distribution

ψ_{min}	η_{exp} (%)	η_{QED} (%)
5°	3.5 ± 1.3	3.6 ± 0.3
10°	2.6 ± 1.1	2.1 ± 0.3
20°	1.7 ± 0.9	1.1 ± 0.3

IV.3. Mu pair production.

For the reaction $e^+e^- \rightarrow \mu^+\mu^-$ we give in table 4 twice the lowest order cross section. Because of the symmetry of the cross section around $\theta = 90^\circ$ we only tabulate it for angles up to 90° .

Table 4

$2d\sigma^0/d\Omega_+$ for mu pair production, for different values of the beam energy, P_{+0} (in GeV) and the scattering angle θ .

P_{+0} θ	1.0	2.0	3.0	5.0
5°	5.14	1.29	0.57	0.21
20°	4.86	1.22	0.54	0.20
40°	4.10	1.03	0.46	0.16
60°	3.24	0.81	0.36	0.13
85°	2.62	0.66	0.29	0.10
90°	2.61	0.65	0.29	0.10

We will first consider the case where the charges of the muons are not measured. As for Bhabha scattering we allow a maximum acollinearity of 10° and a threshold energy of 0.2 GeV. We find the following corrections for δ_S . These are symmetric around $\theta = 90^\circ$.

Table 5

The radiative corrections (in %) to mu pair production (no charge measurement), for different values of the beam energy, P_{+0} (in GeV), and the scattering angle θ ; the acollinearity angle $\zeta = 10^\circ$, and the threshold energy $E_{th} = 0.2$ GeV.

P_{+0} θ	1.0		2.0		3.0		5.0	
	δ_A	δ_T	δ_A	δ_T	δ_A	δ_T	δ_A	δ_T
5°	-6.0	5.5 ± 0.6	-7.0	6.6 ± 0.7	-7.5	7.1 ± 0.8	-8.2	8.0 ± 0.8
20°	-6.0	0.5 ± 0.3	-7.0	0.7 ± 0.4	-7.5	0.8 ± 0.4	-8.2	0.9 ± 0.5
40°	-6.0	-2.7 ± 0.2	-7.0	-2.8 ± 0.2	-7.5	-2.9 ± 0.2	-8.2	-2.9 ± 0.3
60°	-6.0	-4.3 ± 0.1	-7.0	-4.6 ± 0.1	-7.5	-4.8 ± 0.1	-8.2	-5.0 ± 0.2
90°	-6.0	-5.1 ± 0.1	-7.0	-5.5 ± 0.1	-7.5	-5.7 ± 0.1	-8.2	-5.9 ± 0.1

The numbers listed in the row δ_A are the corrections if one assumes the validity of the soft photon approximation. In this case the maximum photon energy is taken to be the energy corresponding to k_1 in the Dalitz plot of fig. 6 (chapter III).

The soft photon approximation yields a contribution which is (almost) independent of the angle θ , whereas the full contribution from hard photon emission changes this picture considerably. For small θ hard photon emission gives important contributions.

This can be understood as follows: if θ is small, the region of strong peaking of the matrix element squared lies close to the border of the Dalitz plot and hence a large part of it is in the allowed region of phase space.

If the charges of the muons are measured we will assume that also the energies of the outgoing particles can be determined. We therefore assume that an event contributes to the cross section if $q_{\pm 0} \geq p_{+0} - \epsilon$. In table 6, ϵ is taken such that the muons have at least 90% of the maximum energy. We tabulate separately the corrections which are even in $\cos \theta$, (δ_S) and the corrections which are odd in $\cos \theta$, (δ_D).

Table 6

The percentage corrections δ_S and δ_D for mu pairs production for different values of the beam energy, p_{+0} (in GeV), and the scattering angle θ ; the threshold energy $E_{th} = 0.9 p_{+0}$.

$\theta \backslash p_{+0}$	1.0		2.0		3.0		5.0	
	δ_S	δ_D	δ_S	δ_D	δ_S	δ_D	δ_S	δ_D
5°	-10.0	14.0	-11.6	15.8	-12.6	16.4	-13.7	16.6
20°	-9.8	8.0	-11.4	8.1	-12.4	8.1	-13.6	8.2
40°	-9.2	4.3	-10.8	4.3	-11.7	4.3	-12.9	4.3
60°	-8.2	2.2	-9.7	2.2	-10.7	2.2	-11.7	2.2
85°	-6.6	0.3	-7.8	0.3	-8.5	0.3	-9.7	0.3

(all numbers are ± 0.1)

In this case the shape of the allowed photon phase space is such that now around $\theta = 90^\circ$ the hard photons contribute considerably to the correction.

One may wonder whether approximate calculations reproduce these results. As can be seen from table 5 the soft photon approximation differs considerably from the exact calculation. Even if the soft photon expression (III-72) is

integrated over the full phase space large differences occur. It has also been suggested that it would suffice to consider radiation from the electrons only. In the case of no charge detection this changes δ_A and δ_N up to 50%. In this specific situation these changes almost cancel, but one could imagine situations in which only the isotropic phase space would contribute, and then the changes in δ_T would be considerable.

Finally results for the acoplanarity are presented in table 7. We tabulate $2d\sigma/d\psi$ for a beam energy of 2.0 GeV other conditions are the same as for Bhabha scattering.

Table 7

The acoplanarity distribution (in nb) for mu pair production for a beam energy of 2 GeV, a threshold energy of 0.2 GeV, $\theta_{\min} = 45^\circ$, $\theta_{\max} = 135^\circ$.

ψ	$2 \frac{d\sigma}{d\psi}$
5°	1.28
10°	0.46
20°	0.14
40°	0.04
60°	0.02
90°	0.01
120°	0.01
150°	0.02
180°	0.06

IV.4. Two gamma production.

For the reaction $e^+e^- \rightarrow \gamma\gamma$ we present a table of the lowest order cross section. Because this cross section is symmetric around $\theta = 90^\circ$ (like in the muon case) only values of θ up to 90° are tabulated.

Then using the same criteria as for Bhabha scattering we give the corrections in table 9.

Finally the acoplanarity distribution is given in table 10. The calculations for this reaction have been taken from [9].

Table 8

The lowest order cross section (in nb) for two gamma production for different values of the beam energy, p_{+0} (in GeV), and the scattering angle, θ .

$\theta \backslash p_{+0}$	1.0	2.0	3.0	5.0
5°	1360	339.9	151.1	54.39
20°	83.45	20.86	9.27	3.34
40°	19.91	4.98	2.21	0.80
60°	8.64	2.16	0.96	0.35
90°	5.18	1.30	0.58	0.21

Table 9

The radiative corrections (in %) for two gamma production for different values of the beam energy, p_{+0} (in GeV) and the scattering angle θ . The acollinearity angle $\zeta = 10^\circ$, and the threshold energy $E_{th} = 0.2$ GeV.

$\theta \backslash p_{+0}$	1.0	2.0	3.0	5.0
5°	11.3 ± 0.8	15.2 ± 1.0	17.7 ± 1.2	19.0 ± 1.4
20°	-0.1 ± 0.3	-0.2 ± 0.4	-0.3 ± 0.4	-0.3 ± 0.4
40°	-4.2 ± 0.2	-4.6 ± 0.2	-5.0 ± 0.2	-5.2 ± 0.2
60°	-5.9 ± 0.1	-6.4 ± 0.1	-6.8 ± 0.1	-7.3 ± 0.1
90°	-6.7 ± 0.1	-7.4 ± 0.1	-7.8 ± 0.1	-8.3 ± 0.1

IV.5. Conclusions.

For future Q.E.D. experiments with e^+e^- colliding beams at high energies and accuracies at the level of a few percent, the full radiative corrections to order α^3 have to be taken into account. In particular when two body events are selected by the criterion that they are back to back, quite hard photons can be emitted. The exact matrix elements for hard photon emission have to be used.

Table 10

The acoplanarity distribution (in nb) for two gamma production for a beam energy of 2 GeV, a threshold energy of 0.2 GeV, $\theta_{\min} = 45^\circ$, and $\theta_{\max} = 135^\circ$.

ψ	$d\sigma/d\psi$
5°	1.94
10°	0.77
20°	0.32
40°	0.15
60°	0.11
90°	0.08
120°	0.07
150°	0.07
180°	0.06

In this thesis a flexible method is given to calculate radiative corrections for colliding beam experiments. Within this method different experimental situations can be easily represented. This method has actually been applied in a specific experiment (Bhabha scattering) [2]. The experimental results indicate that at 2.0 GeV and 2.5 GeV there is a good agreement with theory.

APPENDIX A

A.1. In this appendix conventions, Feynman rules and cross section formulae, used in this thesis are summarized.

Contravariant four-vectors are denoted by $k^\mu = (k^0, k^1, k^2, k^3) = (k^0, \vec{k})$. The diagonal elements of the metric tensor are given by $g_{00} = -g_{11} = -g_{22} = -g_{33} = 1$, all other elements are zero. The notation for inner products of four-vectors and three-vectors is (pq) and $\vec{p} \cdot \vec{q}$ respectively. For derivatives we use $\partial_\mu \equiv \frac{\partial}{\partial x^\mu}$.

A.2. The spin $-\frac{1}{2}$ fermions e and μ are described by means of the Dirac equation.

$$(-i\gamma^\mu \partial_\mu + m)\psi(x) = 0. \quad (\text{A.1})$$

The 4×4 matrices γ^μ satisfy the anti-commutation relations.

$$\{\gamma^\mu, \gamma^\nu\} = 2g^{\mu\nu} \cdot \mathbb{1}, \quad \gamma^0 \gamma^\mu \gamma^0 = \gamma^{\mu*} \quad *) \quad (\text{A.2})$$

where $\mathbb{1}$ is the unit matrix. For the contraction of four-vectors with γ -matrices we write $p_\mu \gamma^\mu = \not{p}$, furthermore we define $\gamma^5 = i\gamma^0 \gamma^1 \gamma^2 \gamma^3$.

A specific representation can be given with the help of the 2×2 Pauli matrices

$$\sigma_1 = \begin{pmatrix} 0 & 1 \\ 1 & 0 \end{pmatrix}, \quad \sigma_2 = \begin{pmatrix} 0 & -i \\ i & 0 \end{pmatrix}, \quad \sigma_3 = \begin{pmatrix} 1 & 0 \\ 0 & -1 \end{pmatrix} \quad (\text{A.3})$$

We have (each entry is a 2×2 matrix)

$$\gamma^0 = \begin{pmatrix} \mathbb{1} & 0 \\ 0 & -\mathbb{1} \end{pmatrix}, \quad \gamma^k = \begin{pmatrix} 0 & \sigma_k \\ -\sigma_k & 0 \end{pmatrix}, \quad k = 1, 2, 3. \quad (\text{A.4})$$

In actual calculations we need the following trace formulae.

*) + means herm. conjugate.

$$\begin{aligned}
\text{Tr} \mathbb{1} &= 4, \\
\text{Tr} \gamma^5 &= 0, \\
\text{Tr} \not{a} \not{b} &= 4(ab), \\
\text{Tr} \not{a} \not{b} \not{c} \not{d} &= 4[(ab)(cd) + (ad)(bc) - (ac)(bd)], \\
\text{Tr} \not{a}_1 \not{a}_2 \dots \not{a}_{2n} &= \text{Tr} \not{a}_{2n} \not{a}_{2n-1} \dots \not{a}_2 \not{a}_1, \\
\text{Tr} \gamma^5 \not{a} \not{b} &= 0, \\
\text{Tr} \gamma^5 \not{a} \not{b} \not{c} \not{d} &= 4i \epsilon_{\alpha\beta\gamma\delta} a^\alpha b^\beta c^\gamma d^\delta,
\end{aligned} \tag{A.5}$$

here $\epsilon_{\alpha\beta\gamma\delta}$ is the totally anti-symmetric tensor ($\epsilon_{0123} = 1$). Furthermore the trace of an odd number of γ 's disappears. In the reduction of products one often uses,

$$\begin{aligned}
\gamma_\mu \not{a} \gamma^\mu &= -2\not{a}, \\
\gamma_\mu \not{a} \not{b} \gamma^\mu &= 4(ab), \\
\gamma_\mu \not{a} \not{b} \not{c} \gamma^\mu &= -2\not{c} \not{b} \not{a}.
\end{aligned} \tag{A.6}$$

The plane wave solutions of the Dirac equation are characterised by the spinors $u(\vec{p}, s)$ and $v(\vec{p}, s)$, $s = 1, 2$,

$$\begin{aligned}
u(\vec{p}, s) &= \left(\frac{m + \omega(\vec{p})}{2m} \right)^{\frac{1}{2}} \begin{pmatrix} \phi_s \\ \frac{\vec{p} \cdot \vec{\sigma}}{m + \omega(\vec{p})} \phi_s \end{pmatrix}, \\
v(\vec{p}, s) &= \left(\frac{m + \omega(\vec{p})}{2m} \right)^{\frac{1}{2}} \begin{pmatrix} \frac{\vec{p} \cdot \vec{\sigma}}{m + \omega(\vec{p})} \phi_s \\ \phi_s \end{pmatrix},
\end{aligned} \tag{A.7}$$

$$\omega(\vec{p}) = \sqrt{\vec{p}^2 + m^2}.$$

In these expressions, ϕ_s are eigenvectors of σ_3 with eigenvalues $+1$ ($s = 1$) and -1 ($s = 2$). The spinors $u(\vec{p}, 1)$ and $v(\vec{p}, 2)$ correspond to electrons and positrons which have (in their rest frame) a spin component $+\frac{1}{2}$ in the z-direction. The other two have spin component $-\frac{1}{2}$ along the z-direction.

The Pauli adjoint of a spinor is given by $\bar{\psi} = \psi^\dagger \gamma^0$. In summing over polarisations we need

$$\sum_{s=1}^2 u(\vec{p}, s) \bar{u}(\vec{p}, s) = (\not{p} + m)/2m,$$

$$\sum_{s=1}^2 v(\vec{p}, s) \bar{v}(\vec{p}, s) = -(\not{p} + m)/2m. \quad (\text{A.8})$$

The fermion field operator is given by

$$\begin{aligned} \psi(x) = & \frac{1}{(2\pi)^{3/2}} \int d^3p \left(\frac{m}{\omega(\vec{p})}\right)^{1/2} \sum_{s=1}^2 b(\vec{p}, s) u(\vec{p}, s) e^{-i(px)} \\ & + d^+(\vec{p}, s) v(\vec{p}, s) e^{i(px)}, \end{aligned} \quad (\text{A.9})$$

$$p_0 = \omega(\vec{p}).$$

The operators b , d , b^+ , d^+ are annihilation and creation operators for electrons and positrons fulfilling

$$\begin{aligned} \{b(\vec{p}, s), b^+(\vec{p}', s')\}_+ &= \delta_{ss'} \delta^3(\vec{p} - \vec{p}'), \\ \{d(\vec{p}, s), d^+(\vec{p}', s')\}_+ &= \delta_{ss'} \delta^3(\vec{p} - \vec{p}'). \end{aligned} \quad (\text{A.10})$$

All other anti-commutators vanish.

The propagator is given by

$$S_F(x) = \frac{1}{(2\pi)^4} \int d^4p S_F(p) e^{-i(px)}, \quad (\text{A.11})$$

$$S_F(p) = \frac{i(\not{p} + m)}{p^2 - m^2 + i\epsilon}.$$

A.3. The photon field operator is given by

$$A^\mu(x) = \frac{1}{(2\pi)^{3/2}} \int \frac{d^3k}{(2k_0)^{1/2}} \sum_{\lambda=0}^3 \epsilon^\mu(\vec{k}, \lambda) [a(\vec{k}, \lambda) e^{-i(kx)} + a^+(\vec{k}, \lambda) e^{i(kx)}], \quad (\text{A.12})$$

$$\text{where } k_0 = |\vec{k}|.$$

The photon annihilation and creation operators a and a^+ fulfil

$$[a(\vec{k}, \lambda), a^+(\vec{k}', \lambda')] = -g^{\lambda\lambda'} \delta(\vec{k} - \vec{k}'), \quad (\text{A.13})$$

all other commutators (also those with fermion operators) vanish.

(B.4) The propagator is given by

$$D_{F\mu\nu}(x) = \frac{1}{(2\pi)^4} \int d^4k D_{F\mu\nu}(k) e^{-i(kx)} \quad (\text{A.14})$$

$$D_{F\mu\nu}(k) = \frac{-ig_{\mu\nu}}{k^2 + i\epsilon}.$$

The polarisation vectors are given by

$$\begin{aligned} \epsilon^\mu(\vec{k}, 0) &= (1, 0, 0, 0), \\ \epsilon^\mu(\vec{k}, 1) &= (0, \vec{\epsilon}(\vec{k}, 1)), \\ \epsilon^\mu(\vec{k}, 2) &= (0, \vec{\epsilon}(\vec{k}, 2)), \\ \epsilon^\mu(\vec{k}, 3) &= (0, \vec{k}/|\vec{k}|), \end{aligned} \quad (\text{A.15})$$

where $\vec{\epsilon}(\vec{k}, 1)$, $\vec{\epsilon}(\vec{k}, 2)$ and $\vec{k}/|\vec{k}|$ form an orthonormal set in three-space. For sums over transverse polarisations, we may use

$$\sum_{\lambda=1}^2 \epsilon^\mu(\vec{k}, \lambda) \epsilon^\nu(\vec{k}, \lambda) \Rightarrow -g^{\mu\nu}, \quad (\text{A.16})$$

provided the photons are coupled to conserved currents, which is the case in QED.

A.4. The scattering of particles is described by the invariant amplitude M , which is a scalar under Lorentz transformations. In quantum electrodynamics, the amplitude M is found if one sums the contributions of all graphs for a specific process. We get

$$M = eM^{(1)} + e^2M^{(2)} + \dots \quad (\text{A.17})$$

where $M^{(k)}$ contains the contributions of graphs with k vertices.

In order to calculate $e^k M^{(k)}$ we have the following rules.

1° For incoming fermions and outgoing anti-fermions we have the factors

$$u(\vec{p}, s) \quad \begin{array}{c} \longrightarrow \\ p^+ \end{array}$$

$$v(\vec{p}, s) \quad \begin{array}{c} \longleftarrow \\ p^+ \end{array}$$

(C1.6)

2° For outgoing fermions and incoming anti-fermions we have the factors

$$\bar{u}(\vec{p}, s) \quad \begin{array}{c} \longrightarrow \\ p \end{array}$$

$$\bar{v}(\vec{p}, s) \quad \begin{array}{c} \longleftarrow \\ p \end{array}$$

3° For incoming or outgoing photons we have a factor

$$\epsilon^\mu(\vec{k}, \lambda) \quad \begin{array}{c} \text{~~~~~} \\ k \end{array}$$

4° Internal fermion lines get

$$\frac{i(\not{p} + m)}{p^2 - m^2 + i\epsilon} \quad \begin{array}{c} \longrightarrow \\ p \end{array}$$

5° Internal photon lines get

$$\frac{-ig_{\mu\nu}}{k^2 + i\epsilon} \quad \begin{array}{c} \text{~~~~~} \\ k \end{array}$$

6° Vertices get a factor

$$-i\gamma^\mu \quad \begin{array}{c} \diagup \quad \diagdown \\ \gamma^\mu \\ \text{~~~~~} \end{array}$$

7° Internal momenta are fixed by four-momentum conservation at the vertices. Free momenta are integrated over. Each momentum integration gets a factor $(2\pi)^{-4}$.

8° Closed fermion loops get - Trace. The trace is to be taken over spinor indices.

A.5. With the invariant amplitude we can calculate cross sections by means of the formula

$$d\sigma = \frac{1}{|v_1 - v_2|} \frac{m_1}{\omega(p_1)} \frac{m_2}{\omega(p_2)} |M|^2 (2\pi)^4 \delta^4(p_1 + p_2 - q_1 - \dots - q_n) d\Omega(q_1) \dots d\Omega(q_n) \quad (\text{A.18})$$

Here we assumed that the two incoming particles are fermions. The volume elements have the following form

$$d\Omega(q_i) = \begin{cases} \frac{d^3 q_i}{(2\pi)^3 2q_{i0}} & \text{if the } i^{\text{th}} \text{ particle is a boson} \\ \frac{m_i d^3 q_i}{q_{i0}} & \text{if the } i^{\text{th}} \text{ particle is a fermion.} \end{cases}$$

If polarisations are not measured, $|M|^2$ has to be averaged over initial polarisations and summed over final polarisations.

where $\bar{u}(k, \lambda)$, $\bar{v}(k, \lambda)$ and $u(k, \lambda)$, $v(k, \lambda)$ are the spinors for the incoming and outgoing particles, respectively, and $\lambda = \pm 1/2$ for fermions and $\lambda = 0, 1$ for bosons.

provided the photons are summed over, which is done in the following way:

4.4. The summation over polarisations is performed by using the following identity:

$$\sum_{\lambda} \epsilon_{\mu\nu\alpha\beta} \epsilon^{\mu\nu\gamma\delta} = 2(\delta_{\alpha\gamma} \delta_{\beta\delta} - \delta_{\alpha\delta} \delta_{\beta\gamma})$$

4.5. Closed fermion loops get a factor -1 . The trace is to be taken over spinor indices. A trace of a product of n gamma matrices is zero if n is odd.

of the formula

$$\text{Tr}(\gamma_5 \gamma_{\mu_1} \gamma_{\mu_2} \dots \gamma_{\mu_n}) = 0 \quad \text{if } n \text{ is odd}$$

$$\text{Tr}(\gamma_5 \gamma_{\mu_1} \gamma_{\mu_2} \gamma_{\mu_3} \gamma_{\mu_4}) = 4i \epsilon_{\mu_1 \mu_2 \mu_3 \mu_4}$$

APPENDIX B

B.1. In this appendix the evaluation of the Feynman integrals and the bremsstrahlung integrals for the mu-pair case will be given. These integrals can all be expressed in terms of logarithms and dilogarithms. The dilogarithm is defined as follows [18].

$$\text{Li}_2(z) = -\int_0^z \frac{\log(1-y)}{y} dy, \quad (z \text{ complex}). \quad (\text{B.1})$$

Due to the multivaluedness of the integrand, this is a multivalued function. We take a branch cut along the real axis from +1 to +∞.

The following integral (for which we write U_{ij} in the following)

$$U(\eta_0, \eta_1, y_i, y_j) = \int_{\eta_0}^{\eta_1} \frac{\log|y - y_j|}{y - y_i} dy, \quad (\text{B.2})$$

(all arguments of U are real) can be expressed in terms of dilogarithms as follows:

$$U_{ij} = \text{Re} \left(\text{Li}_2 \left(\frac{\eta_0 - y_i}{y_j - y_i} \right) - \text{Li}_2 \left(\frac{\eta_1 - y_i}{y_j - y_i} \right) \right) + \log|y_i - y_j| \cdot \log \left| \frac{\eta_1 - y_i}{\eta_0 - y_i} \right|, \quad i \neq j, \quad (\text{B.3})$$

$$U_{ii} = \frac{1}{2} (\log|\eta_1 - y_i|)^2 - \frac{1}{2} (\log|\eta_0 - y_i|)^2.$$

B.2. The integral I.

Using the Feynman parametrisation and performing the k -integration, we find

$$I = -i\pi^2 \int_0^1 2y dy \int_0^1 dx \frac{1}{2(y^2 p_x^2 + (1-y)\lambda^2)}. \quad (\text{B.4})$$

In this expression we introduced

$$p_x = (1 - x)p_+ - xp_- . \quad (\text{B.5})$$

If we neglect terms of order λ , the y integration yields

$$I = -i\pi^2 \int_0^1 \frac{dx}{2p_x^2} \log\left(\frac{p_x^2}{\lambda^2}\right) . \quad (\text{B.6})$$

We now introduce a new variable ϕ by

$$s = 4m^2 \sin^2 \phi , \quad (0 < s < 4m^2) \Rightarrow (0 < \phi < \frac{\pi}{2}) . \quad (\text{B.7})$$

For physical values of s , i.e. $s > 4m^2$ we have to make an analytic continuation. In this physical region we find

$$\phi = \frac{1}{2}(\pi - i \log b) ; \quad (\text{B.8})$$

where we introduced

$$b = \frac{1 - a}{1 + a} , \quad a = (1 - 4m^2/s)^{\frac{1}{2}} . \quad (\text{B.9})$$

We now change integration variables in (B.6).

$$2x - 1 = \frac{\text{tg } \xi}{\text{tg } \phi} . \quad (\text{B.10})$$

With this substitution one easily finds

$$I = \frac{-2i\pi^2}{m^2 \sin^2 2\phi} \left[\phi \log \frac{m}{\lambda} + \int_0^\phi \xi \text{tg} \xi d\xi \right] . \quad (\text{B.11})$$

B.3. The integral I_μ .

In the same way we arrived at (B.4) we find

$$I_\mu = -i\pi^2 \int_0^1 \frac{dx}{p_x} P_{x\mu} . \quad (\text{B.12})$$

If we now use the same substitutions as for I we immediately arrive at

$$I_{\mu} = I_{\Delta} \Delta_{\mu} ; I_{\Delta} = \frac{-2i\pi^2 \phi}{\sin 2\phi} . \quad (B.13)$$

B.4. The integral $I_{\mu\nu}$.

If we use the Feynman parametrisation and perform a shift in the k integration we find

$$I_{\mu\nu} = \int_0^1 2y dy \int_0^1 dx \int d^4k \frac{\frac{1}{2} g_{\mu\nu} (k^2 - y^2 p_x^2) + \frac{1}{2} g_{\mu\nu} y^2 p_x^2 + y^2 p_{x\mu} p_{x\nu}}{(k^2 - y^2 p_x^2)^3} . \quad (B.14)$$

Here we used the fact that the symmetry of the integrand allowed the replacement $k_{\mu} k_{\nu} \rightarrow \frac{1}{2} g_{\mu\nu} k^2$. We now split up the integral in two terms.

$$I_{\mu\nu} = I_{\mu\nu}^{(1)} + I_{\mu\nu}^{(2)}$$

$$I_{\mu\nu}^{(1)} = \frac{1}{2} g_{\mu\nu} \int_0^1 2y dy \int_0^1 dx \int d^4k \frac{1}{(k^2 - y^2 p_x^2)^2} ,$$

$$I_{\mu\nu}^{(2)} = \int_0^1 2y dy \int_0^1 dx \int d^4k \frac{\frac{1}{2} g_{\mu\nu} y^2 p_x^2 + y^2 p_{x\mu} p_{x\nu}}{(k^2 - y^2 p_x^2)^3} . \quad (B.15)$$

The integral $I_{\mu\nu}^{(1)}$ is ultraviolet divergent. We "calculate" $I_{\mu\nu}^{(1)}$ by subtracting and adding an infinite constant.

$$I_{\Lambda} = \int d^4k \frac{1}{(k^2 - \Lambda^2)^2} . \quad (B.16)$$

If we use the substitutions (B.7) and (B.10) the integrals $I_{\mu\nu}^{(1,2)}$ can be evaluated and we find

$$I_{\mu\nu}^{(1)} = \frac{1}{2} g_{\mu\nu} [I_{\infty} + 2i\pi^2 (1 - \phi \cotg \phi)] ,$$

$$I_{\mu\nu}^{(2)} = \frac{-i\pi^2}{8} g_{\mu\nu} - \frac{i\pi^2 \phi}{m^2 \sin 2\phi} \Delta_{\mu} \Delta_{\nu} - \frac{i\pi^2}{2m^2 \sin^2 \phi} (1 - \phi \cotg \phi) p_{\mu} p_{\nu} , \quad (B.17)$$

where $I_{\infty} = I_{\Lambda} + i\pi^2 - i\pi^2 \log(m^2/\Lambda^2)$.

B.5. Vacuum polarization.

We will now look at the amplitude M^C defined in (III-34). From this

expression we take the following integral.

$$\Pi_{(P^2, m^2)}^{\mu\nu} = \frac{-i\alpha}{4\pi^3} \int d^4k \frac{\text{Tr}[\gamma^\mu(\not{P} + \not{k} + m)\gamma^\nu(-\not{P} + \not{k} + m)]}{(m_+)(m_-)}, \quad (\text{B.18})$$

where (m_\pm) were defined in (III-36). The integral (B.18) is divergent. Due to these divergences it is not clear that $\Pi^{\mu\nu}$ fulfils $P_\mu \Pi^{\mu\nu} = 0$ as it should [3]. If we use the Pauli-Villars method of regularisation, gauge invariance can be secured in all steps of the calculation [20].

We define

$$\Pi_{\text{Reg}}^{\mu\nu}(P^2, m^2) = \sum_{i=1}^N c_i \Pi^{\mu\nu}(P^2, m_i^2), \quad (\text{B.19})$$

where the constants c_i are chosen such that

$$\sum_{i=1}^N c_i = 0, \quad \text{and} \quad \sum_{i=1}^N c_i m_i^2 = 0, \quad (\text{B.20})$$

$$c_1 = 1, \quad m_1 = m.$$

In the final result we let $m_i \rightarrow \infty$ for $i = 2, \dots, N$. By means of the Feynman parameter trick and a shift in the k -integration we find

$$\Pi_{\text{Reg}}^{\mu\nu} = \frac{-i\alpha}{4\pi^3} \sum_{i=1}^N c_i \int_0^1 dx \int d^4k \frac{2P_\mu P_\nu - 2P_{\mu\nu} P_{\mu\nu} - g_{\mu\nu}(P^2 - P_x^2 + m_i^2 - \frac{1}{2}k^2)}{(k^2 + P^2 - P_x^2 - m_i^2 + i\epsilon)^2} \quad (\text{B.21})$$

where $P_x = (1 - 2x)P$.

$$\Pi_{\text{Reg}}^{\mu\nu} = 4(P^\mu P^\nu - g^{\mu\nu} P^2) \Pi^{(1)} + 4g^{\mu\nu} \Pi^{(2)}, \quad (\text{B.22})$$

where

$$\Pi^{(1)} = \frac{-i\alpha}{4\pi^3} \sum_{i=1}^N c_i \int_0^1 dx \int d^4k \frac{8(x - x^2)}{(k^2 + 4P^2(x - x^2) - m_i^2 + i\epsilon)^2}, \quad (\text{B.23})$$

$$\Pi^{(2)} = \frac{-i\alpha}{4\pi^3} \sum_{i=1}^N c_i \int_0^1 dx \int d^4k \frac{4P^2(x - x^2) - m_i^2 + \frac{1}{2}k^2}{(k^2 + 4P^2(x - x^2) - m_i^2 + i\epsilon)^2}.$$

Due to the conditions (B.20), $\Pi^{(2)}$ is identically zero. This can be seen by using the following identities,

$$\sum_{i=1}^N c_i \int d^4k \frac{[1, m_i^2, k^2]}{(k^2 - m_i^2)^2} = -i\pi^2 \sum_{i=1}^N c_i [1, m_i^2, 2m_i^2] \log m_i^2. \quad (\text{B.24})$$

As a consequence we have $P_\mu^{\mu\nu} = 0$. By the same argument as used for the vertex correction, we obtain the renormalized $\Pi^{\mu\nu}$ by subtracting $\Pi^{\mu\nu}$ at the point $P^2 = 0$. In this difference the limit $m_i \rightarrow \infty$ for $i = 2, \dots, N$ can be taken and we find, using (B.24),

$$\Pi^{\mu\nu} = 4(P^\mu P^\nu - g^{\mu\nu} P^2) \Pi,$$

with

$$\Pi = \frac{i\alpha}{4\pi^3} \cdot -8i\pi^2 \int_0^1 dx (x - x^2) \log \left[1 - \frac{4P^2}{m^2} (x - x^2) \right]. \quad (\text{B.25})$$

If we now apply the substitutions (B.7) and (B.10), (remembering that $4P^2 = s$) we can easily evaluate Π ; we find

$$\Pi = + \frac{\alpha}{\pi} \left\{ \frac{1}{9} - \left(1 + \frac{1}{3} \cot^2 \phi \right) (1 - \phi \cot \phi) \right\} \quad (\text{B.26})$$

With the expression (B.8) for ϕ we can write

$$\Pi = + \frac{\alpha}{\pi} \left\{ \frac{8}{9} - \frac{a^2}{3} + a \left(\frac{1}{2} - \frac{a^2}{6} \right) \left(\frac{i\pi}{2} + \log b \right) \right\}. \quad (\text{B.27})$$

If we now look at (III-34) and the definition of $\Pi^{\mu\nu}$ in (B.18) we see that in order to obtain M^c we have to multiply M with $-\Pi$. *) The contribution to the cross section can thus be obtained by multiplying $d\sigma^0/d\Omega_+$ by $-2\text{Re}\Pi$.

B.6. The integral G.

Using the Feynman parametrisation and performing the k -integration, we find

$$G = -i\pi^2 \int_0^1 dy \int_0^1 dx y / (y^2 p_x^2 + (1-y)\lambda^2), \quad (\text{B.28})$$

where now $p_x = xp_+ + (1-x)q_+$. After the y -integration, we obtain in the limit $\lambda \rightarrow 0$

$$G = - \frac{i\pi^2}{2} \int_0^1 \frac{dx}{p_x} \log \left(\frac{p_x^2}{\lambda} \right) = \frac{-i\pi^2}{2} [A(s, t) \log \frac{s}{\lambda^2} + B(s, t)], \quad (\text{B.29})$$

*) Here we have to use the fact that $P_\mu \bar{v}(p_+) \gamma^\mu u(p_-) = P_\nu \bar{u}(q_-) \gamma^\nu v(q_+) = 0$.

where

$$A(s, t) = \int_0^1 \frac{dx}{p_x^2}, \quad B(s, t) = \int_0^1 \frac{dx}{p_x^2} \log \left(\frac{p_x^2}{s} \right). \quad (\text{B.30})$$

With the help of the functions U_{ij} we can evaluate $B(s, t)$. We find

$$A(s, t) = [\lambda(t, m^2, \mu^2)]^{-\frac{1}{2}} \log \left| \frac{t - \mu^2 - m^2 - [\lambda(t, m^2, \mu^2)]^{\frac{1}{2}}}{t - \mu^2 - m^2 + [\lambda(t, m^2, \mu^2)]^{\frac{1}{2}}} \right| \quad (\text{B.31})$$

$$B(s, t) = A(s, t) \log \left(\frac{-t}{s} \right) + [\lambda(t, m^2, \mu^2)]^{-\frac{1}{2}} \sum_{i,j=1}^2 \rho_i U_{ij}(0, 1, x_i, x_j)$$

with the functions U_{ij} defined in (B.2) and

$$\begin{aligned} x_1 &= \{t + \mu^2 - m^2 + [\lambda(t, \mu^2, m^2)]^{\frac{1}{2}}\} / 2t, \\ x_2 &= \{t + \mu^2 - m^2 - [\lambda(t, \mu^2, m^2)]^{\frac{1}{2}}\} / 2t, \end{aligned} \quad (\text{B.32})$$

$$\rho_i = (+1, -1).$$

(Here $\lambda(x, y, z) = x^2 + y^2 + z^2 - 2xy - 2yz - 2zx$.)

Thus

$$\frac{1}{2\pi^2} \text{Im } G = -\frac{1}{4} [A(s, t) \log \left(\frac{-s}{\lambda^2} \right) + B(s, t)].$$

B.7. The integral F.

Standard methods allow us to write

$$F = i\pi^2 \int_0^1 dx \int_0^1 dy \int_0^1 dz \frac{y^2 z (P^2 + Y^2 + 2C)}{(Y^2 + C)^2}, \quad (\text{B.33})$$

where

$$Y^2 = P^2(1 + 2yz - 4y + 4y^2 - 4y^2 z + y^2 z^2) + y^2 z^2 Q_x^2,$$

$$Q_x = (1 - x)Q + x\Delta, \quad (\text{B.34})$$

$$C = P^2(2yz - 1).$$

The y integration is readily done, yielding

$$\begin{aligned}
 F = i\pi^2 \int_0^1 dx \int_0^1 dz z \left\{ \frac{1}{z^2 p_x^2 - s(z-1)} - \frac{1}{2z^2 p_x^2 [z^2 p_x^2 - (z-1)s]} \right\} \\
 + i\pi^2 \int_0^1 dx \int_0^1 dz z \left\{ \frac{s(2-z)}{2[z^2 p_x^2 - (z-1)s]^2} \log \frac{z^2 p_x^2}{s(z-1)} \right\}.
 \end{aligned}
 \tag{B.35}$$

Again, p_x has been defined following eq. (B.28). (Note that this p_x differs from the p_x used in the calculation of the vertex integrals.)

Let us call the first term in eq. (B.35) A_1 and the other one A_2 . For A_1 the z -integration gives

$$A_1 = \frac{i\pi^2}{2} \int_0^1 \frac{dx}{p_x} \log \frac{p_x^2}{s} = \frac{i\pi^2}{2} B(s,t)
 \tag{B.36}$$

with the help of (B.29) it also turns out that

$$A_2 = -\frac{\pi^3}{2} A(s,t),
 \tag{B.37}$$

so that

$$\frac{1}{2\pi^2} \text{Im } F = \frac{1}{2} B(s,t).
 \tag{B.38}$$

B.8. The integrals H_P , H_Δ and H_Q .

The integral H_μ is readily written in the form

$$H_\mu = -i\pi^2 \int_0^1 dx \int_0^1 dy \frac{yP_\mu + y^2 p_{x\mu}'}{y^2 p_x^2 + (1-y)\lambda^2},
 \tag{B.39}$$

where

$$p_x = xp_+ + (1-x)q_+, \quad p_x' = x\Delta + (1-x)Q - P.
 \tag{B.40}$$

Separating the numerator in the three vectors and doing the y -integration, we obtain

$$H_\mu = P_\mu [G + i\pi^2 \int_0^1 \frac{dx}{p_x}] - i\pi^2 \Delta_\mu \int_0^1 \frac{x dx}{p_x} - i\pi^2 Q_\mu \int_0^1 \frac{(1-x) dx}{p_x}
 \tag{B.41}$$

Repeated use of the expression for $A(s,t)$ gives

$$\begin{aligned}
 \frac{1}{2\pi^2} \text{Im } H_P &= \frac{1}{2\pi^2} \text{Im } G + \frac{1}{2} A(s,t), \\
 \frac{1}{2\pi^2} \text{Im } H_\Delta &= -\frac{1}{2} A(s,t),
 \end{aligned}
 \tag{B.42}$$

where

$$\frac{1}{2\pi^2} \text{Im } H_Q = -\frac{1}{2} [A(s, t) - A_x(s, t)] , \quad (B.42)$$

$$A_x(s, t) = \int_0^1 \frac{x dx}{p_x} = [\log \left(\frac{m}{\mu} \right)^2 + (t + \mu^2 - m^2) A(s, t)] / 2t . \quad (B.43)$$

Interchanging m and μ in A_x gives $A - A_x$, exhibiting the symmetry in H_Δ and H_Q .

B.9. The integrals $F_{\Delta, Q}$ and $G_{\Delta, Q}$.

It is clear from the definition of these integrals that F_Q and G_Q can be obtained from F_Δ and G_Δ by replacing $m \rightarrow \mu$. It thus suffices to calculate F_Δ and G_Δ . One easily proves that

$$F_\Delta = \frac{-i\pi^2}{2} \int_0^1 dx \int_0^1 dy \frac{2y}{[y^2(1-2x)^2 P^2 - y^2 P^2 + (1-y^2)m^2 - i\epsilon]} . \quad (B.44)$$

The x -integration yields

$$F_\Delta = \frac{-i\pi^2}{2P^2} \int_0^1 dy \frac{1}{y\sqrt{1-a((1-y)/y)^2}} \log \left| \frac{\sqrt{1-a((1-y)/y)^2} - 1}{\sqrt{1-a((1-y)/y)^2} + 1} \right| \quad (B.45)$$

where $a = (m^2 - i\epsilon)/P^2$. It is profitable now to assume $a < 0$, so that afterwards an analytic continuation has to be made. A change of variables leads to

$$\frac{1}{2\pi^2} \text{Im } F_\Delta = \frac{-2}{s(1-\beta^2)} \int_0^1 \frac{dz \log z}{z^2 + 2z[(1+\beta^2)/(1-\beta^2)] + 1} \quad (B.46)$$

$$\beta = (1 - m^2/P^2)^{\frac{1}{2}} ,$$

which can readily be evaluated in terms of dilogarithms to yield

$$\frac{1}{2\pi^2} \text{Im } F_\Delta = [\text{Li}_2((\beta-1)/(\beta+1)) - \text{Li}_2((\beta+1)/(\beta-1))] / 2s\beta . \quad (B.47)$$

From the definition of G_Δ follows

$$G_\Delta = F_\Delta / \beta^2 + 2 \left\{ \int d^4k / (+)(-) - \int d^4k / (\Delta)(+) \right\} / s\beta^2 , \quad (B.48)$$

which eventually leads to

$$\frac{1}{2\pi^2} \text{Im } G_{\Delta} = \frac{1}{\beta^2} \frac{1}{2\pi^2} \text{Im } F_{\Delta} - \frac{1}{s\beta^2} \log\left(\frac{s}{m^2}\right) . \quad (\text{B.49})$$

B.10. The bremsstrahlung integral.

Using the Feynman trick we find

$$R = \int_{|\vec{k}| < k_1} \frac{d^3k}{k_0} \frac{1}{(p_+ k)(p_- k)} = \int_0^1 dx \int d^3k \frac{1}{(p_x k)^2} , \quad (\text{B.50})$$

with $k_0 = \sqrt{\vec{k}^2 + \lambda^2}$ and where p_x was defined in (B.40). Performing the \vec{k} -integration and omitting terms of order λ gives

$$R = 2\pi \int_0^1 dx [a(x) \log\left(\frac{2k_1}{\lambda}\right)^2 + c(x)] , \quad (\text{B.51})$$

with

$$a(x) = (p_{x0}^2 - |\vec{p}_x|^2)^{-1} ,$$

$$c(x) = a(x) \frac{p_{x0}}{|\vec{p}_x|} \log \frac{p_{x0} - |\vec{p}_x|}{p_{x0} + |\vec{p}_x|} . \quad (\text{B.52})$$

Noting that $p_{x0} = E$ and that

$$(p_x p_x) = t(x^2 - x) + \mu^2(1 - x) + m^2 x , \quad (\text{B.53})$$

we find for the integral $\int_0^1 dx a(x)$, the function $A(s,t)$ which was given in (B.31).

The integral of $c(x)$ is somewhat more involved. Going over to the new integration variable y , defined by

$$[-tx^2 + (t + \mu^2 - m^2)x + E^2 - \mu^2]^{\frac{1}{2}}/E = y - x(-t)^{\frac{1}{2}}/E , \quad (\text{B.54})$$

the integral of $c(x)$ can be evaluated as

$$C(s,t) = \int_0^1 dx c(x) = [\lambda(t, \mu^2, m^2)]^{\frac{1}{2}} \sum_{i,j=1}^4 \epsilon_i \delta_j U(\eta_0, \eta_1, y_i, y_j) . \quad (\text{B.55})$$

We have introduced the symbols

$$\epsilon_i = (+1, -1, -1, +1), \quad \delta_j = (-1, -1, +1, +1) ,$$

$$\begin{aligned}
 \eta_0 &= (1 - \mu^2/E^2)^{\frac{1}{2}}, & \eta_1 &= (1 - m^2/E^2)^{\frac{1}{2}} + (-t)^{\frac{1}{2}}/E, \\
 y_1 &= -1 - \{t + \mu^2 - m^2 - [\lambda(t, \mu^2, m^2)]^{\frac{1}{2}}\}/2E(-t)^{\frac{1}{2}}, \\
 y_2 &= -1 - \{t + \mu^2 - m^2 + [\lambda(t, \mu^2, m^2)]^{\frac{1}{2}}\}/2E(-t)^{\frac{1}{2}}, \\
 y_3 &= y_1 + 2, \\
 y_4 &= y_2 + 2.
 \end{aligned}
 \tag{B.56}$$

Putting all this together we have

$$R = 2\pi[A(s,t)\log\left(\frac{2k_1}{\lambda}\right)^2 + C(s,t)]. \tag{B.57}$$

Using these expressions we can calculate all the integrals occurring in (III-76) and (III-79).

APPENDIX C

In this appendix, the explicit expressions for

$$F_{ij}(p_+, p_-, q_+, q_-, k) = \sum_{\text{spins}} N_i N_j^* \quad (C.1)$$

are given.

In fact, several relations among the functions F_{ij} hold, such that it suffices to know only three of them to know them all, e.g., F_{11} , F_{12} and F_{13} .

From the reality of F_{ij} , it follows that

$$F_{ij} = F_{ji} \quad (C.2)$$

Since in the traces of eq. (C.1) odd powers of m (or μ) are always combined with an odd number of γ matrices, and, therefore, vanish, we can replace m by $-m$ (or μ by $-\mu$) without changing anything. The following relations are then obtained:

$$\begin{aligned} F_{22}(p_+, p_-, q_+, q_-, k) &= F_{11}(p_-, p_+, q_+, q_-, k) \quad , \\ F_{14}(p_+, p_-, q_+, q_-, k) &= -F_{13}(p_+, p_-, q_-, q_+, k) \quad , \\ F_{23}(p_+, p_-, q_+, q_-, k) &= -F_{13}(p_-, p_+, q_+, q_-, k) \quad , \\ F_{24}(p_+, p_-, q_+, q_-, k) &= F_{13}(p_-, p_+, q_-, q_+, k) \quad . \end{aligned} \quad (C.3)$$

Finally, from the similarity between the muon and the electron part, it follows that

$$\begin{aligned} F_{33}(p_+, p_-, q_+, q_-, k) &= F_{11}(q_+, q_-, p_+, p_-, -k) \quad , \\ F_{44}(p_+, p_-, q_+, q_-, k) &= F_{22}(q_+, q_-, p_+, p_-, -k) \quad , \\ F_{34}(p_+, p_-, q_+, q_-, k) &= F_{12}(q_+, q_-, p_+, p_-, -k) \quad . \end{aligned} \quad (C.4)$$

The explicit expressions for F_{11} , F_{12} and F_{13} are

$$\begin{aligned}
 m^2 \mu^2 F_{11} = & -[4m^2 2(p_+q_+)(p_-q_-) + 2(p_+q_-)(p_-q_+) \\
 & - s'(p_+p_-) - s(q_+q_-) + s s'] \\
 & + [4m^2 + 4(kp_-)] [2(p_+q_+)(kq_-) + 2(p_+q_-)(kq_+) \\
 & - 2(q_+q_-)(kp_+) + s'(kp_+)] \\
 & - 4m^2(kp_-) [2(q_+q_-) - 2s'] ,
 \end{aligned}$$

$$\begin{aligned}
 m^2 \mu^2 F_{12} = & 4(p_+p_-) [2(p_+q_+)(p_-q_-) + 2(p_+q_-)(p_-q_+) \\
 & - s'(p_+p_-) - s(q_+q_-) + s s'] \\
 & - 2(p_+p_-) [2(P'q_+)(kq_-) + 2(P'q_-)(kq_+) \\
 & - 2(q_+q_-)(kP')] \\
 & - 2(kP') [2(p_+q_+)(p_-q_-) + 2(p_+q_-)(p_-q_+) \\
 & - s(q_+q_-) + s s' - 2m^2 \mu^2] \\
 & - 8m^2(kq_+)(kq_-) + 8(kp_+)(p_-q_+)(p_-q_-) \\
 & + 8(kp_-)(p_+q_+)(p_+q_-) ,
 \end{aligned} \tag{C.5}$$

$$\begin{aligned}
 m^2 \mu^2 F_{13} = & - [4(p_-q_-) - 2(kq_-) + 2(kp_-)] \\
 & [2(p_+q_+)(p_-q_-) + 2(p_+q_-)(p_-q_+) + m^2 s' + \mu^2 s] \\
 & + 2(p_-q_-) [2(p_+q_+)(kq_-) + 2(p_+q_-)(kq_+) + 2\mu^2(kp_+) \\
 & - 2(p_+q_+)(kp_-) - 2(p_-q_+)(kp_+) - 2m^2(kq_+)] \\
 & - 2(kp_-) [2\mu^2(p_+q_+) + s'(p_+q_-)] \\
 & + 2(kq_-) [2m^2(p_+q_+) + s(p_-q_+)] \\
 & + 8(p_+q_+)(kp_-)(kq_-) + 4m^2(kq_+)(kq_-) \\
 & + 4\mu^2(kp_+)(kp_-) ,
 \end{aligned}$$

with

$$P' = p_+ + p_- = 2P .$$

With these expressions, one can now calculate $\Sigma |M^B|^2$ of eq.(III-70). We have verified that, in the charge symmetric $\mu^+ \mu^-$ case, they lead to an expression which coincides with that recently obtained by D'Ettore Piazzoli [19].

APPENDIX D

In order to derive eq. (III-95), one has to solve for q_{+0} from eq. (III-86) when $\cos \delta = z$ and

$$q_{-0} = P_0 - q_{+0} - k. \quad (D.1)$$

By introducing the variable $x = q_{+0}q_{-0}$, one finds the equation

$$x^2(1 - z^2) - 2x(\xi + z^2\mu^2) + \xi^2 + z^2\mu^2(b^2 - \mu^2) = 0, \quad (D.2)$$

with the solutions

$$x = \gamma \pm \left[\gamma^2 - \frac{\xi^2 + z^2\mu^2(b^2 - \mu^2)}{1 - z^2} \right]^{1/2}. \quad (D.3)$$

The quantities γ , ξ , and b have been defined in eqs. (III-96) and (III-97)

From the definition of x and eq. (D.1), one arrives at

$$q_{+0}^2 - b q_{+0} + \gamma \pm \left[\gamma^2 - \frac{\xi^2 + z^2\mu^2(b^2 - \mu^2)}{1 - z^2} \right]^{1/2} = 0. \quad (D.4)$$

By examining the limit $\mu \rightarrow 0$, one finds that the lower sign in eq. (D.4) has to be taken.

References

- [1] C. Bernardini, Proc. 1971 Int. Symposium on Electron and Photon Interactions at High Energies, Cornell University, Ithaca, NY(1971) 38; V. Sidorov, *ibid.*, p. 66.
- [2] H. Newman et al., Phys. Rev. Lett. 32, (1974) 483.
- [3] J.D. Bjorken and S.D. Drell, Relativistic Quantum Mechanics, and Relativistic Quantum Fields, McGraw-Hill, Inc. (New York).
- [4] G. Källén, Handbuch der Physik V/1, ed. S. Flügge (Springer, Berlin, 1958).
- [5] J. Schwinger, Quantum Electrodynamics, Dover Publications, Inc., (New York, 1958).
- [6] B.E. Lautrup, A. Petermann and E. de Rafael, Phys. Reports 3 (1972) 193.
- [7] F. Block and A. Nordsieck, Phys. Rev. 52 (1937) 54.
- [8] D.R. Yennie, S.C. Frautschi and H. Suura, Ann. Phys. (NY) 13 (1961) 379.
- [9] F.A. Berends and R. Gastmans, Nucl. Phys. B61 (1973) 414.
- [10] F.A. Berends, K.J.F. Gaemers and R. Gastmans, Nucl. Phys B57 (1973) 381, Nucl. Phys. B63 (1973) 381, and F.A. Berends, K.J.F. Gaemers and R. Gastmans, Nucl. Phys. B68 (1974) 541.
- [11] Review of Particle Properties, T.A. Lasinski et al., Rev. Mod. Phys. 45 (1973) S1.
- [12] J.E. Augustin et al., Phys. Rev. Lett. 30 (1973) 462.
- [13] I.B. Kriplovich, Novosibirsk preprint 59-72.
R.W. Brown et al., N.A.L. preprint THY-97 (1972),
D.A. Dicus, Univ. of Rochester preprint, UR-420 (1973).
- [14] M.L.G. Redhead, Proc. Roy. Soc. 220A (1953) 219.
R.V. Polovin, Soviet Phys. JETP, 4 (1957) 385.
- [15] S.M. Swanson, Phys. Rev. 154 (1967) 1601.
- [16] B. Lautrup, Proceedings of the 2nd Colloquium on Advanced Computing Methods in Theoretical Physics, Marseille, p. I-58, (1971).
- [17] G. Potzolu, Nuov. Cim. 20 (1961) 542.
- [18] L. Lewin, Dilogarithms and Associated Functions, Macdonald & Co. Inc., (London, 1958).
- [19] B. D'Ettore Piazzoli, CNEN Laboratori Nazionali di Frascati, LNF-71/61 (1971).
- [20] W. Pauli and F. Villars, Rev. Mod. Phys. 21 (1949) 434.
- [21] A. Litke, Thesis (Harvard University, 1970) unpublished.

S A M E N V A T T I N G

In dit proefschrift worden de werkzame doorsneden gegeven tot orde α^3 van de processen

$$e^+ e^- \rightarrow \gamma \gamma ,$$

$$e^+ e^- \rightarrow e^+ e^- ,$$

$$e^+ e^- \rightarrow \mu^+ \mu^- .$$

Kennis van deze werkzame doorsneden is noodzakelijk als men de theorie van electromagnetische interacties (quantum electrodynamica) wil toetsen met behulp van experimenten waarbij men electron- en positronbundels laat botsen.

De theoretische werkzame doorsneden bestaan uit twee bijdragen met een verschillend karakter. In de eerste plaats worden tot op orde α^3 bijdragen gegeven voor bovengenoemde reacties. Deze bijdragen zijn divergent. De divergentie wordt veroorzaakt doordat de massa van het foton nul is en wordt infrarood divergentie genoemd.

Omdat in de genoemde reacties geladen deeltjes versneld worden, kunnen de reacties nooit zuiver „elastisch" zijn en moeten zij vergezeld gaan van de uitzending van extra fotonen (Bremsstrahlung). Deze fotonen kunnen een willekeurig kleine energie hebben en het is daarom experimenteel niet mogelijk om onderscheid te maken tussen b.v. de reactie $e^+ e^- \rightarrow \mu^+ \mu^-$ en de reactie $e^+ e^- \rightarrow \mu^+ \mu^- \gamma$.

Om nu op zinnvolle wijze experiment en theorie te vergelijken, moet bij de werkzame doorsnede van het proces zonder extra foton emissie de werkzame doorsnede gevoegd worden van de reactie met foton emissie. Ook deze bijdrage is infrarood divergent en wel zodanig dat in de som deze divergenties juist tegen elkaar wegvallen. Een probleem is nu om uitgaande van een specifieke experimentele situatie te bepalen welke fotonen niet worden gedetecteerd.

In hoofdstuk II worden enige opmerkingen gemaakt over electromagnetische interacties en worden in laagste orde de werkzame doorsneden voor de drie reacties gegeven. In hoofdstuk III worden voor het proces $e^+ e^- \rightarrow \mu^+ \mu^-$ de berekeningen gegeven van de botsingsdoorsnede tot op orde α^3 terwijl hier bovendien een flexibel formalisme wordt ontwikkeld waarmee de invloed van experimentele condities op de waarneembaarheid van Bremsstrahlung fotonen kan worden geanalyseerd.

In hoofdstuk IV worden resultaten van numerieke berekeningen gegeven. Ook worden hier voor het proces $e^+e^- \rightarrow e^+e^-$ (Bhabha verstrooiing) de theoretische werkzame doorsneden vergeleken met recente experimentele gegevens. Hier blijkt dat er een zeer goede overeenstemming is tussen experiment en theorie.

[2] S. Schwinger et al., Phys. Rev. Lett. 12, (1974) 433.

[3] J.D. Bjorken and S.D. Drell, Relativistic Quantum Fields, McGraw-Hill, Inc. (1964).

[4] S. Klein, Handbuch der Physik VII, ed. S. Flügge (Springer, Berlin, 1958).

[5] J. Schwinger, Quantum Electrodynamics, Dover Publications (New York, 1958).

[6] J. Schwinger, Phys. Rev. 125, 974 (1962).

[7] J. Schwinger, Phys. Rev. 125, 974 (1962).

[8] J. Schwinger, Phys. Rev. 125, 974 (1962).

[9] J. Schwinger, Phys. Rev. 125, 974 (1962).

[10] J. Schwinger, Phys. Rev. 125, 974 (1962).

[11] J. Schwinger, Phys. Rev. 125, 974 (1962).

[12] J. Schwinger, Phys. Rev. 125, 974 (1962).

[13] J. Schwinger, Phys. Rev. 125, 974 (1962).

[14] J. Schwinger, Phys. Rev. 125, 974 (1962).

[15] J. Schwinger, Phys. Rev. 125, 974 (1962).

[16] J. Schwinger, Phys. Rev. 125, 974 (1962).

[17] J. Schwinger, Phys. Rev. 125, 974 (1962).

[18] J. Schwinger, Phys. Rev. 125, 974 (1962).

[19] J. Schwinger, Phys. Rev. 125, 974 (1962).

[20] J. Schwinger, Phys. Rev. 125, 974 (1962).

[21] J. Schwinger, Phys. Rev. 125, 974 (1962).

[22] J. Schwinger, Phys. Rev. 125, 974 (1962).

[23] J. Schwinger, Phys. Rev. 125, 974 (1962).

[24] J. Schwinger, Phys. Rev. 125, 974 (1962).

[25] J. Schwinger, Phys. Rev. 125, 974 (1962).

[26] J. Schwinger, Phys. Rev. 125, 974 (1962).

[27] J. Schwinger, Phys. Rev. 125, 974 (1962).

[28] J. Schwinger, Phys. Rev. 125, 974 (1962).

[29] J. Schwinger, Phys. Rev. 125, 974 (1962).

[30] J. Schwinger, Phys. Rev. 125, 974 (1962).

De tekeningen in dit proefschrift werden vervaardigd door de heer W.F. Tegelaar, het typewerk werd op snelle en accurate wijze verzorgd door mevr. E. de Haas-Walraven.

De „Nederlandse Organisatie voor Zuiver Wetenschappelijk Onderzoek” (ZWO), stelde de auteur in staat om in 1971 de zomerschool te Les Houches te bezoeken.

